International Journal of Plasticity, Vol. 3, pp. 211-247, 1987
Printed in the U.S.A.

0749-6419/87 $3.00 + .00

THE PHYSICS OF PLASTIC DEFORMATION

ELIAS C. AIFANTIS

Michigan Technological University

*Dedicated to the Memory of Aris Phillips**

Abstract—A simplified physical picture is extracted from the many complicated processes occurring during plastic deformation. It is based upon a set of continuously distributed straight edge dislocations, the carriers of plastic deformation, moving along their slip plane, interacting with each other and the lattice, multiplying and annihilating. The principles of continuum physics, that is the conservation laws of mass and momentum, and results from discrete dislocation modelling are then employed to analyze the situation and deduce a closed set of relations describing the evolution of deformation and the associated forces that bring it about. A simple method is suggested for extending these relations to macroscales. This way, current phenomenological models of plasticity are physically substantiated. Moreover, a framework is provided for rigorously constructing small and large deformation theories of plasticity. Finally, a new possibility is made available for capturing the salient features of the heterogeneity of plastic flow including the wavelength of persistent slip bands, the width of shear bands, and the velocity of Portevin-Le Chatelier bands.

I. INTRODUCTION

Plastic deformation, as any other physical process, can be best understood by considering and properly analyzing the underlying mechanisms responsible for it. While several such mechanisms, including twinning, void growth, grain boundary sliding and phase transformations, may be envisioned, we single out the most important and simplest of them all: dislocation motion and evolution. Dislocations, however, are complex geometric objects and they reveal themselves indirectly through the electron microscope as "edges," "screws," "loops," "dipoles," "tangles" or "forests." Moreover, they do not just travel carrying deformation along, but they can also stop, multiply and annihilate. Their spatial distribution evolves neither isotropically nor uniformly. Instead, they move along specific slip planes in preferred slip directions, and they exhibit an ability to organize themselves in periodic layers, hexagonal and other ordered structures, in analogy to living systems. Such a trend to self-organization or symmetry breaking is a result of the competition between spatial gradients modelling dislocation motion/interaction, and nonlinearities modelling dislocation generation/annihilation.

It is thus evident that the development of a physical theory of plastic deformation is

*It is an honor and pleasure to have been given the opportunity to dedicate this article to Aris Phillips, not only because through his own research he set a permanent example for young scientists, in general, but also because he was a constant supporter of my earlier work on the mechanics and physics of diffusion in solids, in particular. In line with the great Greek tradition, he was an advocate of geometry, but he did not fail to recognize the importance of the analysis of the physical processes that bring geometric changes about. In fact, at the time that the majority of the mechanics journals showed hesitation towards new approaches to stress-assisted diffusion, environmental fracture and dislocation-based plasticity theories, Phillips' "Acta Mechanica" became a vehicle for the dissemination of such ideas and helped their growth and maturity.

faced with two difficult problems: consideration of the complex geometries involved, and analysis of the nonlinear processes governing the evolution of dislocated state. Over the last fifty years much knowledge has been accumulated concerning the mechanical behavior of "single dislocations" or "dislocation arrays" within the limitations of linear theory of elasticity (see, for example, HIRTH & LOTHE [1982]). Similarly, substantial progress has been accomplished in the understanding of the group behavior of "continuously distributed dislocations" in an attempt to derive a dislocation-based theory of plasticity (see, for example, MURA [1982]). In these studies, considerable emphasis was put on the geometric details pertaining to dislocation configurations, but less attention was paid to the physics of dislocation reactions and inelastic forces associated with their motion. In fact, continuous distributions of dislocation theories seem to require an *a priori* specification of quantities such as the dislocation density and flux tensors in order to draw conclusions for the induced plastic deformation.

In parallel to the rigorous geometric approaches for both discrete and continuous distributions of dislocations, there has been another set of developments, commonly known as "dislocation dynamics" (see, for example, GILMAN [1969]). It is exclusively concerned with one-dimensional deductions, but it does not require an *a priori* specification of the dislocation distribution in order to calculate plastic strains. Despite the simplifications introduced in this approach, which is most popular among solid state physicists, it seems that it correlates well with experimental data pertaining to one-dimensional tests. Thus, while in one dimension it can predict interesting phenomena such as upper and lower yield points and describe complicated stress-strain graphs, it is not designed for analyzing three-dimensional situations and guiding the construction of macroscopic theories of plasticity.

The conclusion that dislocation theory has helped greatly in the qualitative understanding of the microscopic features of plastic deformation, but not as much in guiding the derivation of macroscopic plasticity relations, is apparent in several contributions; see, for example, the review article by Ronald de Wit, contained in a recent volume edited by AIFANTIS & HIRTH [1985]. In the same volume some new approaches to dislocations including "gauge theories" and "field theories of defects" were also discussed, but, again, their applicability to plasticity was not of concern.

It appears from the above discussion that there currently exists a great deal of pessimism concerning the plausibility of utilizing dislocation concepts to construct macroscopic theories of plasticity. The purpose of the present article is to advance a less pessimistic point of view and establish results that, in this author's opinion, deserve attention not only in their own right but also in connection with generating a more optimistic picture about the possibility of deriving useful plasticity relations directly from dislocation considerations. This is attempted by searching for a compromise between the "geometric" theories of continuous distributions of dislocations and the "physical" theories of dislocation dynamics. In contrast to the continuously distributed dislocations approach, there is no need now to *a priori* assume the dislocation density and flux tensors or to neglect the important process of dislocation generation and annihilation. It is necessary, however, to assume much simpler geometries in order to extract useful information from such types of complex physical analyses. Also in contrast to the dislocation dynamics approach which cannot escape its one-dimensional setting, it is now possible to discuss dislocation phenomena of even greater complexity within a three-dimensional framework. While such a new approach to dislocations was suggested a few years ago (see, for example, AIFANTIS [1981], BAMMANN & AIFANTIS [1981, 1982]), it was only recently that the potential of the method was more clearly demonstrated (see, for

example, AIFANTIS [1984,1985], WALGRAEF & AIFANTIS [1985]). An account of these developments can be found in two recent review articles by AIFANTIS [1986b,c].

Section II describes briefly the physical framework upon which the newly proposed conservation and constitutive equations for the dislocated state are based. The adoption of simplified geometries, that is the elaboration on a single family of dislocations only, is compensated for by the consideration of dislocation generation/annihilation and inelastic forces not accounted before in theories for continuously distributed dislocations. In the same section, a brief comparison is given between the mathematical structure of this and previous theories, as applied to a single slip system; it is concluded that the present theory is much richer.

Section III discusses the problem of the transition from microscales to macroscales. Instead of attempting to address the "many-body problem" in a dislocation context, by employing various recently proposed, cumbersome and not always physically realistic averaging procedures (for a critical review of the physical relevance of such procedures see DRUCKER [1984]), a much simpler path is suggested. A set of microscopic plasticity relations is easily obtained within the configuration of single slip by properly defining the plastic strain rate tensor in terms of the production/annihilation rate and flux of dislocations, as well as the orientation tensor associated with the slip system under consideration. On formally eliminating the orientation tensor from these relations and assuming that the structure of the resulting equations is preserved during a transition from the microscale to macroscale (scale invariance), it is possible to obtain macroscopic plasticity relations by adjusting the material coefficients. Alternatively, when formal elimination of the microscopic orientation tensor is not possible, the transition is accomplished by replacing it with a macroscopic orientation tensor associated to the directions of the effective stress. It is thus possible to arrive at familiar statements of classical plasticity and viscoplasticity from a microscopic point of view. Similarly, more recent internal variable plasticity models are recovered and microstructurally substantiated.

Section IV considers the formulation of large deformation theories of plasticity, and illustrates, among other things, that the present framework is most suitable for deriving classes of evolutionary behavior for the "back stress" of macroscopic plasticity. Moreover, it clearly shows that in order to preserve the structure of small deformation plasticity theory in large deformations, the evolution of the back stress should be measured not by the Jaumann rate but by a properly defined corotational rate completely determined within the present setting. In particular, these results provide a microscopic substantiation of various phenomenological proposals for the plastic spin recently and independently advanced by DAFALIAS [1983, 1984], LORET [1983] and Onat [1984]. The little understood problem of deformation-induced anisotropy and texture formation is considered as an example of the predictive ability of the present framework. We show that torsionally induced axial strains (free-end cylindrical specimens) as well as torsionally induced axial stresses (fixed-end cylindrical specimens) can indeed be predicted by the theory in agreement with the experimental data of BAILEY *et al.* [1972], HART & CHANG [1982] and WHITE & ANAND [1986].

Finally, in Section V, we include an extended appendix on the heterogeneity of plastic deformation. It is shown that the present framework can provide a new possibility via bifurcation and stability analysis for a quantitative understanding of the fascinating problem of localization of plastic flow at both the micro and macro level. The key issue in such considerations is the admissibility of nonconvex equations of state and the proper introduction of higher-order gradients to stabilize the behavior and allow for the

possibility of patterned solutions. Three important topics of current interest are briefly considered: The wavelength of persistent slip bands (PSBs) formed during the fatigue of monocrystals, the width of shear bands in rigidly plastic materials and the velocity and structure of deformation bands along with the staircase profile of the stress–strain curve occurring during the straining of polycrystalline tensile specimens under constant stress rate in the Portevin–Le Chatelier regime. The results included in this section are presented in a condensed manner, however, sufficient for stimulating the reader to consult with related past and forthcoming publications (e.g. AIFANTIS [1984, 1986a], WALGRAEF & AIFANTIS [1985, 1987], TRIANTAFYLLIDIS & AIFANTIS [1986], ZBIB & AIFANTIS [1987b]).

II. THE DISLOCATED STATE

In this section we give the basic equations defining the evolution of the dislocated state. This is viewed here as the material state made up of atoms highly disturbed from their equilibrium position and confined at the dislocation cores (excited atoms), while atoms outside the cores (normal atoms) comprise as usual the lattice state. For a continuous distribution of dislocations, lattice and dislocated states can thus be considered as separate superimposed continua supporting their own density, velocity and stress, and interacting with each other by exchanging mass and momentum (AIFANTIS [1984, 1985, 1986]).

For the case of one family of dislocations moving along their slip system designated by $(\mathbf{n}, \boldsymbol{\nu})$ with $\mathbf{n}$ denoting the unit normal to the slip plane and $\boldsymbol{\nu}$ the unit vector in the slip direction, the mass and momentum balances for the dislocated state are given by (AIFANTIS [1984–86])

$$\frac{\partial \rho}{\partial t} + \operatorname{div} \mathbf{j} = \hat{c} \ , \qquad \operatorname{div} \mathbf{T}^D = \hat{\mathbf{f}} \ , \tag{1}$$

and the relevant constitutive equations are assumed to be of the form

$$\mathbf{T}^D = t_m \mathbf{M} + t_\nu \boldsymbol{\nu} \otimes \boldsymbol{\nu} + t_n \mathbf{n} \otimes \mathbf{n} \ ,$$

$$\hat{\mathbf{f}} = (\alpha - \gamma\tau + \beta j)\boldsymbol{\nu} + (\alpha_c - \gamma_c \tau_c + \beta_c j_c)\mathbf{n} \ , \tag{2}$$

$$\hat{c} = \hat{c}(\rho, j, \tau, j_c, \tau_c) \ ,$$

In eqn (1) ρ denotes dislocation density, $\mathbf{j}$ dislocation flux and $\mathbf{T}^D$ dislocation stress. The source terms c and $\hat{\mathbf{f}}$ measures the "effective mass" and "momentum" exchange between dislocated and lattice states. Specifically, $\hat{c}$ represents the generation, immobilization or annihilation of dislocations and $\hat{\mathbf{f}}$ includes, among other things, the effects of lattice friction, damping and the Peach–Koehler force acting on a dislocation as a result of the applied stress.

In eqn (2) the orientation tensor $\mathbf{M}$ of the slip system and the glide and climb components j and j_c of the dislocation flux are defined by

$$\mathbf{M} = \tfrac{1}{2}(\mathbf{n} \otimes \boldsymbol{\nu} + \boldsymbol{\nu} \otimes \mathbf{n}) \ , \quad j = \mathbf{j} \cdot \boldsymbol{\nu} \ , \quad j_c = \mathbf{j} \cdot \mathbf{n} \ , \tag{3a}$$

while the glide and climb-like components of the effective resulted stress τ and τ_c are defined respectively by

$$\tau = \mathrm{tr}(\mathbf{T}^L\mathbf{M}) \ , \quad \tau_c = \mathrm{tr}(\mathbf{T}^L\boldsymbol{\nu} \otimes \boldsymbol{\nu}) \ , \tag{3b}$$

where $\mathbf{T}^L$ denotes the stress tensor carried by the lattice and plays the role of an effective stress

$$\mathbf{T}^L = \mathbf{S} - \mathbf{T}^D \ , \tag{4}$$

with S being the total stress. In the absence of dynamic loading effects, the quasi-static equilibrium equations for S is, as usual,

$$\mathrm{div}\,\mathbf{S} = 0. \tag{5}$$

The coefficients (t_m, t_ν, t_n), (α, γ, β), $(\alpha_c, \gamma_c, \beta_c)$ should be regarded, in general, as functions of the variables entering in $(2)_3$ including an additional quantity l representing an internal length scale such as mean free path or average distance travelled by dislocations. For simplicity, however, we will view these coefficients as functions of the density ρ above as this suffices for our purposes. The coefficients (t_m, t_ν, t_n) measure the interaction forces between dislocations and are responsible for the development of internal stress. The coefficients (α, α_c) measure the lattice-dislocation interaction and are responsible for yielding. The coefficients (γ, γ_c) measure the effect of Peach–Koehler force, while (β, β_c) measure the drag associated with dislocation motion and are responsible for internal damping and viscoplastic flow.

We conclude this section with a brief calculation showing explicitly that the present dislocation framework summarized by the conservation and constitutive equations (1) and (2) contains, indeed, the equations of continuously distributed theories of dislocations. The most recent review on this subject is very clearly given by KOSEVICH [1979]. The governing balance equation in this theory is a tensorial differential statement expressing the conservation of Burgers vectors in the form

$$\dot{\boldsymbol{\alpha}} + \mathrm{curl}\,\mathbf{J}^T = 0 \ , \tag{6}$$

where $\boldsymbol{\alpha}$ is the dislocation density tensor, $\mathbf{J}^T$ the transpose of the dislocation flux tensor and $(\mathrm{curl}\,\mathbf{J})_{ij} = \epsilon_{ilm} J_{jm,l}$. For the derivation of eqn (6), small deformations must be assumed and dislocation reactions must be neglected. Moreover, the traditional use of (6) requires specification of $\boldsymbol{\alpha}$ and J as there are no additional statements to provide a closed system of equations.

To proceed further we define $\boldsymbol{\alpha}$ and J of (6) in terms of the quantities ρ and j of the present theory and configuration as follows

$$\boldsymbol{\alpha} = \int (\mathbf{t} \otimes \mathbf{b})\rho \, \mathrm{d}\Omega \ , \quad \mathbf{J} = \int (\mathbf{t} \times \mathbf{j}) \otimes \mathbf{b} \, \mathrm{d}\Omega \ , \tag{7}$$

where* **b** denotes the common Burgers vector of the parallel edge dislocations under consideration, $(\mathbf{b} = |\mathbf{b}|\boldsymbol{\nu})$ and $(\mathbf{t}, \mathrm{d}\Omega)$ denote a unit tangent vector and a solid angle respec-

*Note that time differentiation was interchangeably denoted by either a superimposed dot or a partial derivative as no essential difference between the two is to be assigned for the cases under consideration. Also, the usual indicial notation is adopted when necessary and the symbols $\cdot$, $\times$, $\otimes$ denote inner product, cross product, and dyadic respectively.

tively, such that the product $\rho\, d\Omega$ represents the total number of dislocations passing through a unit area perpendicular to $\mathbf{t}$ and located inside $d\Omega$ around the direction of $\mathbf{t}$. Upon substitution of (7) into (6) we have

$$\int (\dot{\rho} + \operatorname{div} \mathbf{j})(\mathbf{t} \otimes \mathbf{b}) d\Omega = \int ([\operatorname{grad} \mathbf{j}]\mathbf{t} \otimes \mathbf{b}) d\Omega \ , \tag{8}$$

which, on noting that in the present case there is no dislocation flux in the $\mathbf{n}$ and $\mathbf{t}$ directions ($\mathbf{t}$ is the cross product of $\mathbf{n}$ and $\boldsymbol{\nu}$, $\mathbf{t} = \mathbf{n} \times \boldsymbol{\nu}$) and therefore

$$([\operatorname{grad} \mathbf{j}]\mathbf{t}) \otimes \mathbf{b} = (\mathbf{t} \cdot \operatorname{grad} \mathbf{j})\boldsymbol{\nu} \otimes \mathbf{b} = |b| \frac{\partial j}{\partial t} \boldsymbol{\nu} \otimes \boldsymbol{\nu} = 0 \ , \tag{9}$$

it suggests that

$$\int (\dot{\rho} + \operatorname{div} \mathbf{j})(\mathbf{t} \otimes \mathbf{b}) d\Omega = 0 \ , \tag{10}$$

implying, as the domain of integration is arbitrary, that the local balance law as expressed by eqn (1) can be recovered within the structure of continuously distributed dislocations but with the source term $\hat{c}$ lost.

Further insight on the comparison between the two approaches can be gained by considering the rather recent proposal of introducing inelastic forces within the continuous distributions of dislocations structure, as suggested by KOSEVICH [1979],

$$\mathbf{t} \times \mathbf{S}\mathbf{b} - \mathbf{B}\mathbf{v} - \mathbf{f} = 0 \ , \tag{11}$$

that is by directly extending the equation of motion for a single loop from the discrete to the continuous distribution case. As before, $\mathbf{t}$ denotes the tangent and $\mathbf{b}$ the Burgers vector, $\mathbf{S}$ the total stress, $\mathbf{v}$ an average dislocation velocity, $\mathbf{B}$ a microscopic viscosity (tensor or scalar) coefficient and $\mathbf{f}$ a threshold-like force representing the resistance to dislocation motion caused by the discreteness of the lattice. For the present case of parallel edge dislocations gliding on their plane ($\mathbf{n}$) in the slip direction $\boldsymbol{\nu} = \mathbf{b}/|\mathbf{b}|$, we have $\mathbf{t} = \mathbf{n} \times \boldsymbol{\nu}$, and it thus follows that the $\boldsymbol{\nu}$ and $\mathbf{n}$ components of (11) are exactly the $\boldsymbol{\nu}$ and $\mathbf{n}$ components of $\hat{\mathbf{f}}$ in eqn $(2)_2$ with $\mathbf{S}$ replaced by $\mathbf{T}^L$ and an obvious identification of the remaining quantities. In this connection, we remark that interaction forces between dislocations can only be considered in (11) through the total stress $\mathbf{S}$ of the corresponding Peach–Koehler term. In contrast, such effects are accounted for in the momentum balance $(2)_2$ through both the divergence of the dislocation stress $\mathbf{T}^D$ and the threshold-like force terms entering the structure of $\hat{\mathbf{f}}$ through the coefficients (α, α_c).

We thus see that expression (11) is just a balance of forces motivated directly by discrete modelling, while $(1)_2$ supplemented with $(2)_1$ and $(2)_2$ is a continuum mechanics statement of conservation of momentum and brings forward the important stress $\mathbf{T}^D$ which is a direct counterpart of the "back stress" of macroscopic plasticity. It is noted that the dislocation stress $\mathbf{T}^D$, not present in previous continuum dislocation theories, accounts for inelastic forces and dislocation-core effects and plays a central role in the formation and stability of dislocation patterns. This, as shown by AIFANTIS [1985] and WALGRAEF & AIFANTIS [1985], is due to the fact that the divergence of $\mathbf{T}^D$ in $(1)_2$ gen-

erates gradient-dependent terms whose competition with the nonlinear terms generated by $\hat{c}$ in eqn $(2)_3$ leads to dynamical instabilities and provides a mechanism for the nucleation and evolution of dislocation bands and microscopic deformation bands. With respect to the particular point of view that we wish to advance here regarding macroscopic plasticity, it will be shown in Section IV that the presence of $\mathbf{T}^D$ is essential in substantiating nonlinear plasticity models of the kinematic hardening type, and producing physically based expressions for the plastic spin.

III. FROM MICROSCALES TO MACROSCALES

In this section we show how the structure of the "microscopic" equations (1) and (2) can be utilized to obtain "macroscopic" relations of plasticity. The method that we propose is essentially an answer to the questions: What are the "macroscopic" quantities of interest and how do they relate to the "microscopic" quantities of eqns (1) and (2)?

The discussion becomes simpler by noting immediately that macroscopic plasticity theories are usually based on sufficiently large scales over which plastic micro-heterogeneities are smoothed out. Then, it is not unreasonable to assume that the diver gence terms in eqns (1) do not have any influence on the particular question addressed here and can be formally dropped. Also macroscopic plasticity theories are usually based on the assumption of plastic incompressibility. Again, it is not unreasonable to assume that the dislocation processes that bring volume changes about, that is the climb processes, can be neglected from the present considerations. This suggests that the terms with subscript "c" drop from eqn (2). Finally, the coefficient t_ν in the dislocation stress expression $(2)_1$ can be assumed to vanish, as the normal stress $t_\nu(\boldsymbol{\nu} \otimes \boldsymbol{\nu})$, which is mostly responsible for climb, is expected to play a much less significant role than the normal stress $t_n(\mathbf{n} \otimes \mathbf{n})$, which accounts for, among other things, dislocation dipole presence and decomposition. With these simplifications, the microscopic equations to be used for macroscopic deductions have the form

$$\begin{aligned} &\dot{\rho} = \hat{c}(\rho, j, \tau) \ , \quad \hat{f} = \alpha - \gamma\tau + \beta j = 0 \ , \\ &\mathbf{S} = \mathbf{T}^L + \mathbf{T}^D; \quad \mathbf{T}^D = t_m \mathbf{M} + t_n \mathbf{N} \ , \end{aligned} \tag{12}$$

where for convenience we have set $\mathbf{n} \otimes \mathbf{n} = \mathbf{N}$, and also replaced the partial time derivative in (1) with the material time derivative, denoted by a superimposed dot, for the present case of macro-homogeneity and quasistatic considerations.

We are now ready to begin the identification procedure between macroscopic and microscopic quantities. In particular, the microscopic stress quantities $\mathbf{S}$, $\mathbf{T}^L$, and $\mathbf{T}^D$ of $(12)_3$ are assumed to preserve their character and interrelationship during their transition to the macroscale, where they are identified with the macroscopic total stress, macroscopic effective stress and macroscopic back stress respectively. For convenience, we will maintain the same symbols for designating these stress quantities in both scales.

As macroscopic plasticity theories are usually based on a yield condition, we have to identify this feature within the microscopic theory. This is done via the "reduced" equation of motion for the dislocated state $(12)_2$, which can be rewritten as

$$\tau = \kappa + \bar{\kappa} j \ , \tag{13}$$

where

$$\kappa = \alpha/\gamma \quad \text{and} \quad \bar{\kappa} = \beta/\gamma \ .$$

Having thus identified a microscopic yield condition through eqn (13), it remains to define one more central quantity of macroscopic plasticity theory: the plastic strain $\mathbf{E}^p$. In conformity with established results—that the plastic strain rate $\dot{\mathbf{E}}^p$ is a state variable, rather than the strain $\mathbf{E}^p$ itself—we propose the following relationship for it:

$$\dot{\mathbf{E}}^p = \dot{\gamma}^p \mathbf{M} \ , \tag{14}$$

where the orientation factor $\mathbf{M}$ determines the tensorial character of plastic flow and the scalar $\dot{\gamma}^p$ its intensity. As the orientation tensor $\mathbf{M}$ is traceless, eqn (14) reflects the fact that climb processes were neglected and plastic incompressibility was assumed.

To gain further insight into the nature of the scalar measure of plastic flow rate $\dot{\gamma}^p$, it is instructive to consider situations where the definition of the plastic strain itself is meaningful and reasonably quantified in terms of a relatively small number of dislocation parameters (AIFANTIS [1985]):

$$\mathbf{E}^p = \gamma^p(\rho, l)\mathbf{M} \ . \tag{15}$$

This relation may stand on its own right as far as one does not rush to relate it directly to stress or use it in a constitutive equation. In eqn (15) ρ is the dislocation density and l, which as mentioned earlier was suppressed from the constitutive equations (2), denotes an internal length-scale parameter, such as average "flight distance" of dislocations. Upon differentiation, eqn (15) gives

$$\dot{\mathbf{E}}^p = \dot{\gamma}^p \mathbf{M} + \gamma^p \dot{\mathbf{M}} \ , \tag{16}$$

where γ^p is as in (15) and $\dot{\gamma}^p$ may be readily expressed as

$$\dot{\gamma}^p = A\dot{\rho} + Bj \ , \tag{17}$$

with the scalar coefficients A and B defined† by $A = \partial\gamma^p/\partial\rho$ and $B = \partial\gamma^p/\partial l$. Relation (17) clearly shows that, in conservative glide, the plastic flow rate depends on both dislocation production (the $A\dot{\rho}$ term) and dislocation speed (the Bj term). It is worth noting that if we set $A = 0$, then substitution of (17) into (14) yields a direct three-dimensional generalization of Orowan's celebrated equation of dislocation dynamics.

Another important feature revealed from the rate form of (15) is the fact that only when the slip system $(\mathbf{n}, \boldsymbol{\nu})$ remains unchanged (for example, the slip plane does not rotate) with respect to the external fixed system of coordinates, and therefore $\dot{\mathbf{M}}$ vanishes, does eqn (16) reduce to (14). For most of the discussion that follows in this section we will drop the second term of the right-hand side of (16) by either assuming zero material rotation or considering it of "second order" as being the product of two "first-order" terms. In general, $\dot{\mathbf{M}}$ relates to spin terms which, in contrast to linear elasticity, are not usually negligible in plasticity even for small deformation theory. For large plas-

†Alternatively, and certainly more generally and correctly, eqn (17) can be viewed as a constitutive equation rather than a consequence of differentiating the relation $\gamma^p = \gamma^p(\rho, l)$.

tic deformations, of course, the rotation effect and the associated spin is the essence of the theory, and the subject is considered in detail in the next section.

On returning to (14) we view it along with (13) and (12) as the basic vehicle for accomplishing the micro-macro transition. What is still missing, however, is a macroscopic interpretation of the microscopic orientation tensor **M**. To establish such a macroscopic counterpart for **M** we note first that, physically, the product of τj represents a microscopic working or power term due to dislocation motion along their slip plane. It should, therefore, be a nonnegative quantity. In view of the definitions $(3a)_1$, (4) and (14) this observation implies the statement

$$\tau j > 0 \Leftrightarrow (\mathbf{S} - \mathbf{T}^D) \cdot \dot{\mathbf{E}}^p > 0 \ , \tag{18}$$

which could be viewed as a microscopic justification of the well-known statement of plastic irreversibility. In deriving (18) we have assumed, for simplicity, that $A = 0$ and of course $B > 0$. Indeed, (18) may be viewed as the appropriate dissipation or entropy inequality which can motivate the determination of a macroscopic substitute for **M**. Consistently with the macroscopic principle of maximum dissipation for maximum entropy production, we may now search for that **M** which maximizes the left hand side of inequality $(18)_2$ and therefore $(18)_1$. Under the current assumptions, maximizing τj is equivalent to maximizing $\dot{\gamma}^p \tau$, and for a preassigned amount of plastic flow rate $\dot{\gamma}^p$ the system will try to maximize its entropy production by maximizing the orientation-dependent quantity $\tau [\tau = \mathrm{tr}(\mathbf{T}^L \mathbf{M}) = \mathbf{T}^L \cdot \mathbf{M}]$.

The above discussion suggests the following maximization problem for a macroscopic determination of **M**

$$\begin{aligned} \tau &= \max \{\mathrm{tr}(\mathbf{T}^L \mathbf{M})\} \ , \\ \mathrm{tr}\,\mathbf{M} &= 0 \ , \quad \mathrm{tr}\,\mathbf{M}^2 = \tfrac{1}{2} \ , \end{aligned} \tag{19}$$

where the constraints in (19) are a direct consequence of the definition $(3a)_1$. The solution to (19) is obtained through the use of Lagrange multipliers. It gives (Bammann & Aifantis [1982], Aifantis [1984])

$$\tau = \sqrt{J} \ , \quad \mathbf{M} = \frac{\mathbf{T}^{L'}}{2\sqrt{J}} \ , \tag{20}$$

where $\mathbf{T}^{L'}$ denotes the deviatoric part of the effective stress $\mathbf{T}^L$ and J its second invariant

$$J = \tfrac{1}{2}\mathrm{tr}\,\mathbf{T}^{L'^2} \ , \quad \mathbf{T}^{L'} = \mathbf{T}^L - \tfrac{1}{3}(\mathrm{tr}\,\mathbf{T}^L)\mathbf{1} \ . \tag{21}$$

With this determination of **M** it is now possible to derive classes of macroscopic plastic behavior by utilizing directly the basic equations (12), the yield condition (13), and the plastic strain rate equation (14) or (16).

III.1. *Classical plasticity*

Let us assume the conditions that the classical theory of perfect plasticity is based upon, that is zero hardening, rate-insensitivity and constant yield stress. Within our framework, these assumptions can formally be expressed as follows:

$$\hat{c} = 0 \ , \quad \mathbf{T}^D = 0 \ , \quad \bar{\kappa} = 0 \ , \quad \kappa = \mathrm{const} \ . \tag{22}$$

Then upon comparison of (13) and (20) we have

$$J = \kappa^2 \ , \tag{23}$$

the classical Huber–Mises yield criterion, where now J is the second invariant of the deviatoric part of the total stress $J = \frac{1}{2}\mathbf{S}' \cdot \mathbf{S}'$, since the back stress $\mathbf{T}^D$ was assumed to vanish.

Upon substitution of the expression of $\mathbf{M}$ given by $(20)_2$ into definition (14), we have

$$\dot{\mathbf{E}}^p = \frac{\dot{\gamma}^p}{2\sqrt{J}} \mathbf{S}' \ , \tag{24}$$

which, in view of (23) and the relation implied by (14) $\dot{\gamma}^p = \sqrt{2\dot{\mathbf{E}}^p \cdot \dot{\mathbf{E}}^p} = 2\sqrt{II}$ with II denoting the second invariant of $\dot{\mathbf{E}}^p$, becomes

$$\dot{\mathbf{E}}^p = \frac{\sqrt{II}}{\kappa} \mathbf{S}' \ , \tag{25}$$

that is the Prandtl–Reuss flow rule.

III.2. *Classical viscoplasticity*

If we maintain all but one of the assumptions embodied in eqns (22), that is allow for rate-sensitivity effects, we must require

$$\bar{\kappa} \neq 0 \ . \tag{26}$$

Then assuming again, for simplicity, that $A = 0$ in (17) and defining the viscosity coefficient $\eta = \bar{\kappa}/B$, we obtain from the microscopic dynamic yield condition (13) with the use of $(20)_1$ and (14)

$$2\eta \dot{\mathbf{E}}^p = \left(1 - \frac{\kappa}{\sqrt{J}}\right) \mathbf{S}' \ , \tag{27}$$

that is the Hohenemser–Prager viscoplastic flow rule. In turn, the overstress Φ is given by the formula

$$\Phi = \frac{\sqrt{J}}{\kappa} - 1 \tag{28}$$

and the appropriate macroscopic yield condition reads

$$\sqrt{J} = \kappa + 2\eta\sqrt{II} \ . \tag{29}$$

III.3. *Isotropic hardening*

Here we return to the assumption of neglecting rate-sensitive effects but relax the restriction of constant yield or flow stress. We also retain the hypothesis of vanishing back stress, as this is the central feature of isotropic hardening, but let the dislocation production term $\hat{c}$ be different than zero and responsible for the hardening mechanism. Thus, in place of (22) we now have

$$\hat{c} \neq 0 \ , \quad \mathbf{T}^D = 0 \ , \quad \bar{\kappa} = 0 \ , \quad \kappa = \kappa(\rho) \ . \tag{30}$$

We assume, in particular, that the source term $\hat{c}$, whose general form is given by eqn (12), is proportional to the rate of microscopic plastic work τj, which, in turn, is proportional to the macroscopic plastic work, $\mathbf{S}\cdot\dot{\mathbf{E}}^p$. We thus have

$$\hat{c} \propto \tau j \propto \mathbf{S}\cdot\dot{\mathbf{E}}^p \Rightarrow \dot{\rho} = \Lambda \mathbf{S}\cdot\dot{\mathbf{E}}^p \ , \tag{31}$$

where the coefficient Λ is assumed to be constant. On using (31) to change variables in $(30)_2$ and recalling eqn (23), which is also valid for the case of nonconstant κ, we obtain

$$J = \kappa^2 \ , \quad \kappa = \hat{\kappa}(w_p) \ , \quad w_p = \int \mathbf{S}\cdot d\mathbf{E}^p \ , \tag{32}$$

that is the classical statement of isotropic hardening.

III.4. *Kinematic hardening*

Here we consider the effect of plastic anisotropy signified by the nonvanishing of the back stress $\mathbf{T}^D$. For simplicity, we maintain all other assumptions embodied in eqn (22). Then

$$\mathbf{T}^D \neq 0 \ , \tag{33}$$

and the microscopic yield condition (13) with $\bar{\kappa} = 0$, reads

$$\tfrac{1}{2}(\mathbf{S}' - \mathbf{T}^{D'})\cdot(\mathbf{S}' - \mathbf{T}^{D'}) = \kappa^2 \ , \tag{34}$$

where the primes, as usual, denote deviatoric parts and the macroscopic results $(20)_2$ together with $(12)_3$ were used. Condition (34) is the classical yield condition of kinematic hardening.

To complete the description, evolution equations for the back stress $\mathbf{T}^D$ are required. Such equations can be derived from the present microscopic theory by utilizing $(12)_1$ and (14) to formally eliminate the microscopic orientation tensors $\mathbf{M}$ and $\mathbf{N}$ and then, on the basis of the scale invariance argument, assume that the resultant relations hold true at the macroscale. An easy result can immediately be derived by considering that $\mathbf{T}^D$ in $(12)_4$ is deviatoric. Then t_n vanishes and

$$\mathbf{T}^D = t_m \mathbf{M} \ , \tag{35}$$

which also suggests that $\mathbf{T}^D$ and $\dot{\mathbf{E}}^p$ are coaxial. By differentiating (35), neglecting rotation effects ($\dot{\mathbf{M}} = 0$), and using (14) to eliminate $\mathbf{M}$, we obtain with $c = \dot{t}_m/\dot{\gamma}^p$

$$\dot{T}^D = c\dot{\mathbf{E}}^p \ , \tag{36}$$

that is the classical statement of Prager's kinematic hardening rule.

A less familiar hardening rule is obtained by retaining $t_n \neq 0$ and therefore

$$\mathbf{T}^D = t_m \mathbf{M} + t_n \mathbf{N} \ , \tag{37}$$

emphasizing, among other things, that the plastic strain rate $\dot{\mathbf{E}}^p$ and the back stress $\mathbf{T}^D$ are not coaxial. Again, on differentiating (37) and eliminating from the resultant equation the orientation tensors $\mathbf{M}$ and $\mathbf{N}$ with the aid of (14) and (37) we obtain

$$\dot{\mathbf{T}}^D = c\dot{\mathbf{E}}^p - d\mathbf{T}^D \ , \tag{38}$$

where now the coefficients c and d are defined by

$$c = \frac{1}{\dot{\gamma}^p t_n}\,(\dot{t}_m t_n - t_m \dot{t}_n) \ , \quad d = \frac{\dot{t}_n}{t_n} \ . \tag{39}$$

The form of evolution equation (38) is reminiscent of the Armstrong-Frederick evanescent memory hardening rule, and it will be discussed in the next section in conjunction with large deformation theory.

III.5. *Vertex type theories*

Here we show how the present structure can generate a class of plasticity models commonly known as "corner" or "vertex" theories. To accomplish this we start with (16), the complete rate form of (15), without dropping the spin terms associated with $\dot{\mathbf{M}}$. Then on recalling the macroscopic result $(20)_2$, with the assumption of course that $\mathbf{T}^D = 0$, we obtain by direct differentation

$$\dot{\mathbf{M}} = \frac{1}{2\sqrt{J}}\left(\dot{\mathbf{S}}' - \frac{\mathbf{S}'\dot{J}}{2J}\right) \ , \tag{40}$$

which, in view of the definition of $J = \frac{1}{2}\mathbf{S}'\cdot\mathbf{S}'$, gives upon substitution to (16)

$$\dot{\mathbf{E}}^p = \frac{\dot{\gamma}^p}{2\sqrt{J}}\,\mathbf{S}' + \frac{\gamma^p}{2\sqrt{J}}\left[\dot{\mathbf{S}}' - \frac{\mathbf{S}'(\mathbf{S}'\cdot\dot{\mathbf{S}}')}{2J}\right] \ , \tag{41}$$

which is precisely the starting formula of the corner theory of plasticity as reported, for example, by STOREN & RICE [1975].

In concluding this section on small deformation theories of plasticity we remark that the central result contained in formula (20) and utilized excessively in establishing the micro-macro transition, may be cast in slightly more general forms by relaxing the assumptions embodied in the maximization procedure. For example, for "frictional" materials and volume-sensitive cases where the yield condition depends on hydrostatic stress (e.g. metals with voids, soils), it is reasonable to modify the maximization problem (19) as

$$\begin{gathered} \max(\tau - \alpha\sigma_N) = \kappa \ , \\ \operatorname{tr}\mathbf{M} = 0 \ , \quad \operatorname{tr}\mathbf{M}^2 = \tfrac{1}{2} \ , \quad \operatorname{tr}(\mathbf{MN}) = 0 \ , \quad \operatorname{tr}\mathbf{N} = 1 \ , \end{gathered} \tag{42}$$

where τ is as before (with $\mathbf{T}^D = 0$), $\sigma_N = \operatorname{tr}(\mathbf{SN})$, and α a friction-like coefficient. Then, on using again the method of Lagrange multipliers, we can derive

$$\sqrt{J_2'} - \frac{\alpha}{3}\,J_1 = \kappa \ , \tag{43}$$

with J_1 and J_2' denoting the first invariant of stress and second invariant of deviatoric stress, respectively. Condition (43) is precisely the classic result of DRUKER & PRAGER [1952] postulated on strictly macroscopic grounds to solve problems of soil plasticity.

Accordingly, the flow rule (24) is easily modified, but we do not consider this subject further.

IV. LARGE DEFORMATION PLASTICITY

In this section we elaborate on the problem of plasticity at finite strains. It is clearly shown that the present dislocation framework is most suitable for deriving classes of large deformation plasticity theories. Attention is confined to kinematic hardening models where evolution equations for the back stress $\mathbf{T}^D$ are desired. Two outstanding issues, not unrelated to each other, are of considerable interest currently in this area of research: material rotation and the constitutive structure of back stress. Formally, the effect of material rotation is reflected on the type of corotational rate used to measure the evolution of the back stress. Thus, in a certain sense, it may be viewed as being of a constitutive nature not requiring a separate treatment. If it is desired, however, to maintain some degree of continuity in extending a specific constitutive equation, for example Prager's kinematic hardening rule (36), from small to large deformations, then it is necessary to separate the strain rate effect from the material rotation effect.

A mechanism for accomplishing it most conveniently is provided by the structure of single slip as follows. We imagine an observer riding with the slip system which now, in contrast to the small deformation cases considered in the previous section, is rotating with a specific angular velocity depending on the spin of the continuum within which it is embedded, as well as the rate of plastic deformation (or strain rate) and the level of internal stress development (or back stress). It is then natural for this observer to adopt the same constitutive structure as in small deformation theory, where rotation effects are absent, by computing the various field quantities with respect to the rotating frame. The description is completed by developing an appropriate expression for the angular velocity or spin of the slip system with respect to the external fixed axes of coordinates.

The process outlined above is carried out explicitly below where classes of evolutionary behavior for the back stress $\mathbf{T}^D$ are obtained on the basis of microscopic analysis. The results provide a direct physical justification of various phenomenological models previously proposed in the literature on intuitive or experimental grounds, and suggest explicit expressions for the corresponding phenomenological coefficients. Moreover, they readily show the physical relevance of plastic spin and its importance in computing the appropriate corotational rate for the back stress. In particular, the specific constitutive expression for the plastic spin proposed recently and independently by DAFALIAS [1983], LORET [1983] and ONAT [1984] is rigorously derived on microscopic grounds and a micromechanical framework for more general physically based forms is made available.

We begin with some standard kinematic relationships of large-deformation elastoplasticity to set up the background for the subsequent analysis. The multiplicative decomposition of the total deformation gradient $\mathbf{F}$, routinely used in continuum plasticity for the last twenty years but introduced by physicists and dislocation dynamicists over thirty five years ago, is also employed here; however, in a slightly different version

$$\mathbf{F} = \mathbf{R}\mathbf{U}^e\mathbf{F}^p \ , \tag{44}$$

where $\mathbf{R}$ denotes the rotation of the lattice-slip system or material rotation (as opposed to the rotation of the continuum), $\mathbf{U}^e$ is the elastic stretch and $\mathbf{F}^p$ represents the purely

plastic part of the deformation gradient. In usual theories of elastoplasticity the first two terms of the right-hand side of eqn (44) are lumped together and denoted by $\mathbf{F}^e$, the elastic deformation gradient. As this practice may raise some questions concerning the uniqueness of the intermediate relaxed configuration, that is the configuration of the continuum after removal of $\mathbf{F}^e$, we retain decomposition (44) as our starting point. Assigning $\mathbf{R}$ to certain characteristic directions of the material, in this case the lattice or slip directions, it removes the above ambiguity and allows for a clear presentation of the main ideas. Physically, $\mathbf{R}$ arises from the geometric constraints imposed by the boundary conditions on the slip directions, $\mathbf{U}^e$ arises from the usual reversible lattice displacements of elastic nature and $\mathbf{F}^p$ arises from permanent or irreversible slipping of crystal portions with respect to each other due to dislocation motion.

The velocity gradient $\mathbf{L}$ can now be computed via eqn (44) as

$$\mathbf{L} = \dot{\mathbf{F}}\mathbf{F}^{-1} = \dot{\mathbf{R}}\mathbf{R}^T + \mathbf{R}\dot{\mathbf{U}}^e\mathbf{U}^{e-1}\mathbf{R}^T + \mathbf{R}\mathbf{U}^e\dot{\mathbf{F}}^p\mathbf{F}^{p-1}\mathbf{U}^{e-1}\mathbf{R}^T \tag{45}$$

On recalling the unique decomposition of $\mathbf{L}$ to its symmetric part or stretching $\mathbf{D}$ and antisymmetric part or vorticity $\mathbf{W}$ (the spin of the continuum)

$$\mathbf{L} = \mathbf{D} + \mathbf{W} \ , \tag{46}$$

and denoting the symmetric and antisymmetric parts of the various second-order tensors in eqn (45) by subscripts "s" and "a," respectively, we have

$$\mathbf{D} = \mathbf{D}^e + \mathbf{D}^p \ , \quad \mathbf{W} = \boldsymbol{\omega} + \mathbf{W}^e + \mathbf{W}^p \ , \tag{47}$$

where

$$\begin{aligned} &\boldsymbol{\omega} = \dot{\mathbf{R}}\mathbf{R}^T \ , \quad \mathbf{D}^e = (\mathbf{R}\dot{\mathbf{U}}^e\mathbf{U}^{e-1}\mathbf{R}^T)_s \ , \quad \mathbf{W}^e = (\mathbf{R}\dot{\mathbf{U}}^e\mathbf{U}^{e-1}\mathbf{R}^T)_a \ , \\ &\mathbf{D}^p = (\mathbf{R}\mathbf{U}^e\dot{\mathbf{F}}^p\mathbf{F}^{p-1}\mathbf{U}^{e-1}\mathbf{R}^T)_s \ , \quad \mathbf{W}^p = (\mathbf{R}\mathbf{U}^e\dot{\mathbf{F}}^p\mathbf{F}^{p-1}\mathbf{U}^{e-1}\mathbf{R}^T)_a \ . \end{aligned} \tag{48}$$

Relations (48) indicate, among other things, that for pure plastic deformations ($\mathbf{U}^e = \mathbf{1}$), the elastic stretching and spin vanish ($\mathbf{D}^e = \mathbf{W}^e = 0$) but the spin of the slip system or material spin $\boldsymbol{\omega}$ is clearly different than zero and adds up with the plastic spin $\mathbf{W}^p$ to give the total spin of the continuum or vorticity $\mathbf{W}$.

Even though the above analysis was directly motivated by the configuration of single slip, the derived kinematic relations may be viewed as holding in general, provided that the physical meaning assigned to each one of the terms in eqn (44) is adjusted according to the particular underlying mechanism of elastoplastic deformation. Returning to the present case of single slip we need to further elaborate on the identification of the material spin $\boldsymbol{\omega}$ with the spin of the slip system $(\mathbf{n}, \boldsymbol{\nu})$. First we note that this identification implies

$$\dot{\boldsymbol{\nu}} = \boldsymbol{\omega}\boldsymbol{\nu} \ , \quad \dot{\mathbf{n}} = \boldsymbol{\omega}\mathbf{n} \ , \tag{49}$$

which, in turn, give

$$\dot{\mathbf{M}} = \boldsymbol{\omega}\mathbf{M} - \mathbf{M}\boldsymbol{\omega} \ , \quad \dot{\mathbf{N}} = \boldsymbol{\omega}\mathbf{N} - \mathbf{N}\boldsymbol{\omega} \ . \tag{50}$$

Relations (49) and (50) clearly show that the corotational rate of all orientation quantities with respect to the rotating slip system vanish identically, that is

$$\begin{aligned} &\mathring{\boldsymbol{\nu}} = \dot{\boldsymbol{\nu}} - \boldsymbol{\omega}\boldsymbol{\nu} = 0 \ , \quad \mathring{\mathbf{n}} = \dot{\mathbf{n}} - \boldsymbol{\omega}\mathbf{n} = 0 \ , \\ &\mathring{\mathbf{M}} = \dot{\mathbf{M}} - \boldsymbol{\omega}\mathbf{M} + \mathbf{M}\boldsymbol{\omega} \ , \quad \mathring{\mathbf{N}} = \dot{\mathbf{N}} - \boldsymbol{\omega}\mathbf{N} + \mathbf{N}\boldsymbol{\omega} \ , \end{aligned} \tag{51}$$

suggesting that rotation effects can formally be suppressed if the constitutive equations, for example the evolution equation for the back stress $\mathbf{T}^D$, are expressed with respect to the rotating frame.

To see this more explicitly let us recall the constitutive equation for the back stress (37)

$$\mathbf{T}^D = t_m\mathbf{M} + t_n\mathbf{N} \ , \tag{52}$$

whose material differentiation gives

$$\dot{\mathbf{T}}^D = (\dot{t}_m\mathbf{M} + \dot{t}_n\mathbf{N}) + (t_m\dot{\mathbf{M}} + t_n\dot{\mathbf{N}}) \ , \tag{53}$$

which in view of eqns (50) and (52) becomes

$$\dot{\mathbf{T}}^D = (\dot{t}_m\mathbf{M} + \dot{t}_n\mathbf{N}) + (\boldsymbol{\omega}\mathbf{T}^D - \mathbf{T}^D\boldsymbol{\omega}) \ ,$$

and, on defining the corotational rate $\mathring{\mathbf{T}}^D$ of the back stress by

$$\mathring{\mathbf{T}}^D = \dot{\mathbf{T}}^D - \boldsymbol{\omega}\mathbf{T}^D + \mathbf{T}^D\boldsymbol{\omega} \ , \tag{54}$$

we have

$$\mathring{\mathbf{T}}^D = \dot{t}_m\mathbf{M} + \dot{t}_n\mathbf{N} \ . \tag{55}$$

This suggests that the corotational rate $\mathring{\mathbf{T}}^D$ is given by exactly the same constitutive expression as $\dot{\mathbf{T}}^D$ obtained from (52) or (53) by neglecting the rotation effect ($\dot{\mathbf{M}} = \dot{\mathbf{N}} = 0$). In turn, this shows that for large deformations the rotation effect is most conveniently incorporated by computing the rate of back stress corotationally with the slip system, while maintaining the same constitutive structure as in the case of small deformations where rotation effects are neglected.

To proceed further we assume that the unit vector in the slip direction $\boldsymbol{\nu}$ is attached to the continuum so that its instantaneous angular velocity can be computed from the well-known formula of continuum mechanics

$$\dot{\boldsymbol{\nu}} = (\mathbf{D} + \mathbf{W})\boldsymbol{\nu} - (\boldsymbol{\nu}\cdot\mathbf{D}\boldsymbol{\nu})\boldsymbol{\nu} \ , \tag{56}$$

holding for the rate, with respect to fixed axes of coordinates, of any unit material filament $\boldsymbol{\nu}$. In view of eqn $(49)_1$ and a rearrangement of eqn (56) we can easily show that

$$\boldsymbol{\omega} = \mathbf{W} - [(\boldsymbol{\nu}\otimes\boldsymbol{\nu})\mathbf{D} - \mathbf{D}(\boldsymbol{\nu}\otimes\boldsymbol{\nu})] \ , \tag{57}$$

providing a relation between the spin of the slip system $\boldsymbol{\omega}$ (spin of the material), the vorticity $\mathbf{W}$ (spin of the continuum), and the stretching tensor $\mathbf{D}$ (strain rate). Then, on recalling (47) we can conclude that the elastic and plastic spins $\mathbf{W}^e$ and $\mathbf{W}^p$ are given by the expressions

$$\mathbf{W}^e = (\boldsymbol{\nu} \otimes \boldsymbol{\nu})\mathbf{D}^e - \mathbf{D}^e(\boldsymbol{\nu} \otimes \boldsymbol{\nu}) \ , \quad \mathbf{W}^p = (\boldsymbol{\nu} \otimes \boldsymbol{\nu})\mathbf{D}^p - \mathbf{D}^p(\boldsymbol{\nu} \otimes \boldsymbol{\nu}) \ . \tag{58}$$

In what follows we will assume small elastic deformations so that elastic spin effects are negligible and thus $\mathbf{W}^e = 0$. Then eqn $(47)_2$ gives

$$\boldsymbol{\omega} = \mathbf{W} - \mathbf{W}^p \ , \tag{59}$$

where, as before, the plastic spin $\mathbf{W}^p$ is determined by the direction of anisotropy $(\boldsymbol{\nu})$ and the rate of plastic deformation

$$\mathbf{W}^p = (\boldsymbol{\nu} \otimes \boldsymbol{\nu})\mathbf{D}^p - \mathbf{D}^p(\boldsymbol{\nu} \otimes \boldsymbol{\nu}) \ . \tag{60}$$

This is the place to introduce an explicit relation for the rate of the plastic deformation $\mathbf{D}^p$. The most straightforward extension of eqn (14) from small to large deformations is

$$\mathbf{D}^p = \dot{\gamma}^p \mathbf{M} \ . \tag{61}$$

Then, in view of the definition of $\mathbf{M}$ $(3a)_1$, we obtain upon substitution of eqn (61) into (60)

$$\mathbf{W}^p = \dot{\gamma}^p \boldsymbol{\Omega} \ , \quad \boldsymbol{\Omega} = \tfrac{1}{2}(\boldsymbol{\nu} \otimes \mathbf{n} - \mathbf{n} \otimes \boldsymbol{\nu}) \ . \tag{62}$$

This is precisely the expression for the plastic spin postulated in usual theories of crystal plasticity and was shown here to be a consequence of standard kinematic arguments in conjunction with the constitutive equation (61) for $\mathbf{D}^p$.

Next we derive a macroscopic relation for the plastic spin $\mathbf{W}^p$ by eliminating the orientation tensor $\boldsymbol{\Omega}$ from eqn (62) via the use of expressions (52) and (61) for the back stress $\mathbf{T}^D$ and the plastic strain rate $\mathbf{D}^p$. The result is

$$\mathbf{W}^p = -t_n^{-1}(\mathbf{T}^D\mathbf{D}^p - \mathbf{D}^p\mathbf{T}^D) \ , \tag{63}$$

which provides a microscopic derivation of a proposal advanced recently on phenomenological grounds by DAFALIAS [1983], LORET [1983] and ONAT [1984]. The derivation (63) was first obtained in a joint work by Dafalias and Aifantis (see Appendix of AIFANTIS [1986c]). In fact, more details on various aspects discussed in this section can be found in forthcoming articles by DAFALIAS & AIFANTIS [1987] and ZBIB & AIFANTIS [1987a].

Having a constitutive representation for the plastic spin $\mathbf{W}^p$ readily available, we can explicitly make use of eqn (55) for the evolution of back stress $\mathbf{T}^D$. Indeed, the same arguments that led to eqn (38) can be employed here to derive its large-deformation counterpart. This is precisely the form given by (38) with $\dot{\mathbf{E}}^p$ replaced by $\mathbf{D}^p$, $\dot{\mathbf{T}}^D$ replaced by $\mathring{\mathbf{T}}^D$, and the coefficients c and d still given by (39). Finally, the macroscopic representation for the orientation tensor $\mathbf{M}$ as given by eqn (20) still holds for the finite theory, leading again, through (61), to the flow rule (24) with $\dot{\mathbf{E}}^p$ replaced by

$\mathbf{D}^p$ and $\mathbf{S}'$ with $\mathbf{S}' - \mathbf{T}^{D'}$. On collecting the above results, we have the following central equations for macroscopic plasticity at finite deformations

$$\mathbf{D}^p = \frac{\dot{\gamma}^p}{2\sqrt{J}}(\mathbf{S}' - \mathbf{T}^{D'}) ,$$

$$\mathbf{W}^p = \left(-\frac{1}{t_n}\right)(\mathbf{T}^D\mathbf{D}^p - \mathbf{D}^p\mathbf{T}^D) , \tag{64}$$

$$\mathring{\mathbf{T}}^D = \left(\frac{\dot{t}_m}{\dot{\gamma}^p} - \frac{\dot{t}_n}{t_n}\frac{t_m}{\dot{\gamma}^p}\right)\mathbf{D}^p + \left(\frac{\dot{t}_n}{t_n}\right)\mathbf{T}^D ,$$

signifying, among other things, that not only a constitutive equation for the symmetric part of the plastic velocity gradient $\mathbf{D}^p$ is necessary but also for its antisymmetric part $\mathbf{W}^p$. Moreover, the rate of the back stress $\mathbf{T}^D$ should be taken corotationally with the spin $\boldsymbol{\omega} = \mathbf{W} - \mathbf{W}^p$, that is the difference between the vorticity or total spin of the continuum and the plastic spin.

Various classes of kinematic hardening behavior can now be constructed on the basis of the rigorously derived macroscopic plasticity relations (64) as follows

IV.1. *Model 1*

$t_n = -1/\zeta$, ζ = constant. Then eqns $(64)_3$ and $(64)_2$ imply

$$\mathring{\mathbf{T}}^D = \left(\frac{\dot{t}_m}{\dot{\gamma}^p}\right)\mathbf{D}^p , \quad \mathbf{W}^p = \zeta(\mathbf{T}^D\mathbf{D}^p - \mathbf{D}^p\mathbf{T}^D) , \tag{65}$$

that is, the appropriate extension of Prager's kinematic hardening rule to large deformations and a corresponding expression for the plastic spin with constant coefficient. The set of eqns (65) is essentially the model utilized by DAFALIAS [1983,1984] and more extensively by LORET [1983] to suppress undesirable oscillations occurring in the simple shear problem when the Jaumann rate $\overset{\circ}{\mathbf{T}}{}^D$ instead of $\mathring{\mathbf{T}}^D$ is used.

IV.2. *Model 2*

$\dot{t}_n = -c_n\dot{\gamma}^p t_n$, $\dot{t}_m = -c_n\dot{\gamma}^p t_m + k\dot{\gamma}^p$; $\{c_n, k\}$ = constants. Upon direct integration the above formulae yield

$$t_n = -\frac{1}{\zeta}\,\mathrm{e}^{-c_n\gamma^p} , \quad t_m = \frac{k}{c_n} + \frac{1}{\zeta^*}\,\mathrm{e}^{-c_n\gamma^p} , \tag{66}$$

where ζ and ζ^* are constants of integration. Upon substitution of (66) into $(64)_3$ and $(64)_2$ we have

$$\mathring{\mathbf{T}}^D = k\mathbf{D}^p - c_n\dot{\gamma}^p\mathbf{T}^D , \quad \mathbf{W}^p = \zeta\mathrm{e}^{c_n\gamma^p}(\mathbf{T}^D\mathbf{D}^p - \mathbf{D}^p\mathbf{T}^D) . \tag{67}$$

The set of eqns (67) is essentially the model derived and utilized by DAFALIAS & AIFANTIS [1987] through a less direct method. It is worthwhile noting that $(67)_1$ is precisely the Armstrong–Frederick evanescent memory kinematic hardening rule properly extended to account for large deformation and rotation effects. We see, moreover, that this microscopic derivation suggests that such type of evanescent memory is coupled with an exponential form for the phenomenological coefficient in the expression for the

plastic spin as given by eqn $(67)_2$, rather than the constant coefficient suggested by $(65)_2$.

IV.3. *Model 3*

$\dot{t}_n = -(c_n\dot{\gamma}^p\tau^D)t_n$, $\dot{t}_m = -(c_n\dot{\gamma}^p\tau^D)t_m + k\dot{\gamma}^p$. We remark that all symbols above are as in Model 2 and the new quantity τ^D denotes the second invariant of back stress defined as usual by

$$\tau^D = \sqrt{\tfrac{1}{2}\mathbf{T}^D\cdot\mathbf{T}^D} \ . \tag{68}$$

Roughly speaking, this model suggests that the evolution of the coefficients t_n and t_m is proportional to the degree of internal dissipation due to the action of internal stress itself. It follows that eqn $(64)_3$ becomes

$$\mathring{\mathbf{T}}^D = k\mathbf{D}^p - c_n\dot{\gamma}^p\tau^D\mathbf{T}^D \ , \tag{69}$$

which is reminiscent of the form of the evolution equation suggested by NAGTEGAAL & DE JONG [1982] and BAMMANN [1984]. The expression for the plastic spin is still given by eqn $(64)_2$, where the determination of the coefficient t_n is now coupled with that of $\mathbf{T}^D$ and $\dot{\gamma}^p$ through the evolution equation

$$\dot{t}_n + (c_n\dot{\gamma}^p\tau^D)t_n = 0 \ . \tag{70}$$

More details on these models and numerical solutions of simple example problems including comparisons with experimental data from torsion–tension tests are given in a forthcoming paper by ZBIB & AIFANTIS [1987a]. Nevertheless, we include here for completeness a representative set of theoretical predictions pertaining to two types of exper-

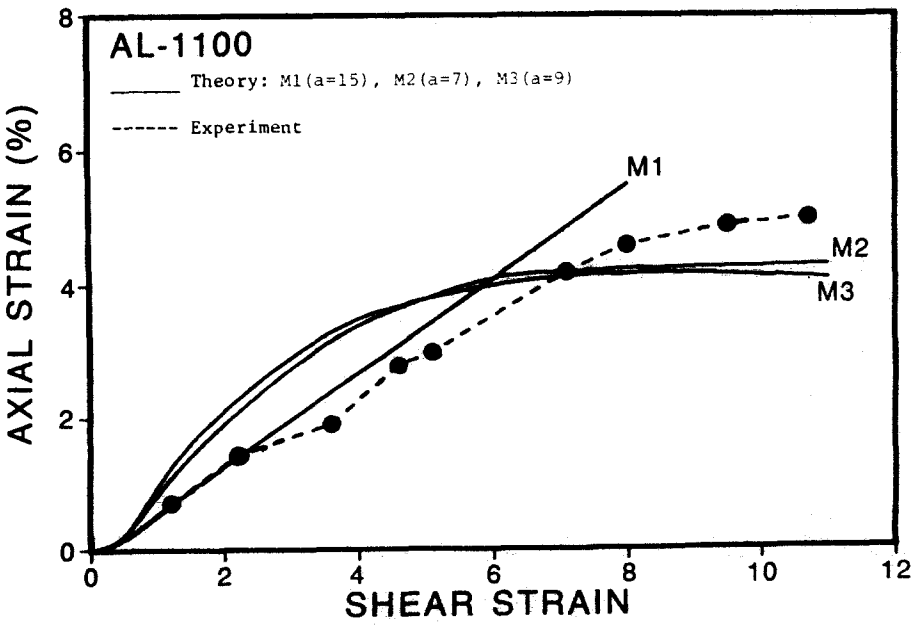

Fig. 1. Axial strain development during torsion of Al-1100 cylindrical bars.

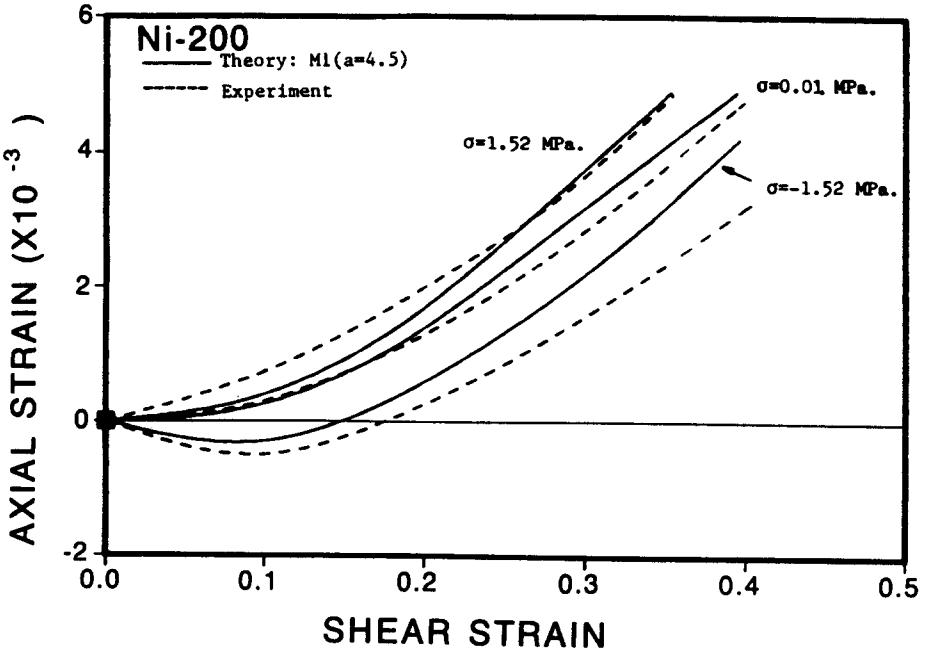

Fig. 2. Axial strain development during tension-torsion of Ni-200 cylindrical bars.

iments: axial strain development due to torsion of free-end cylindrical specimens, and axial stress development due to torsion of fixed-end cylindrical specimens. The axial strain development is shown in Figs. 1 and 2, where theory and experiment are compared for A1-1100 and Ni-200, respectively. The axial stress development is shown in Fig. 3, where theory and experiment are compared for A1-1100. All three models M1 through M3 are used in relation to the Bailey *et al.* data shown in Fig. 1. Only the first model M1 is used in relation to Hart and Chang's data shown in Fig. 2 and White and Anand's data shown in Fig. 3.

The consistency condition [i.e. $\dot{f} = 0; f = (\mathbf{S}' - \mathbf{T}^{D'}) \cdot (\mathbf{S}' - \mathbf{T}^{D'}) - 2\tau^2 = 0$] was used along with the relations (64) for the complete evaluation of the models. It easily turns out that this condition leads to the expression

$$\dot{\gamma}^p = \frac{\mathring{\mathbf{S}}' \cdot (\mathbf{S}' - \mathbf{T}^D)}{\tau(t'_m + 2\tau')} \,, \tag{71}$$

where the prime $'$ in the tensorial quantities $\mathbf{S}$ and $\mathbf{T}^D$ denotes, as usual, deviatoric part, while in the scalar quantities t_m and τ it denotes derivative ($t'_m = \mathrm{d}t_m/\mathrm{d}\gamma^p$, $\tau' = \mathrm{d}\tau/\mathrm{d}\gamma^p$). The strain rate-related parameters of the models, such as the strain hardening modulus‡ $h = \mathrm{d}\bar{\sigma}/\mathrm{d}\bar{\epsilon}$ and the constants (k, c_n), are evaluated with the aid of the stress–strain curve in tension (e.g. $\dot{t}_m/\dot{\gamma}^p = \mathrm{d}t_m/\mathrm{d}\gamma^p = 2h/3 - 2\tau'$), while the spin-related parameter $\zeta (\equiv a/\sigma_y$, σ_y = yield stress) is obtained with the aid of torsion data. For each set of experimental data depicted in Figs. 1–3, the stress–strain curve was fitted by the expressions

‡$\bar{\sigma}$ and $\bar{\epsilon}$ denote effective or equivalent stress and strain, respectively.

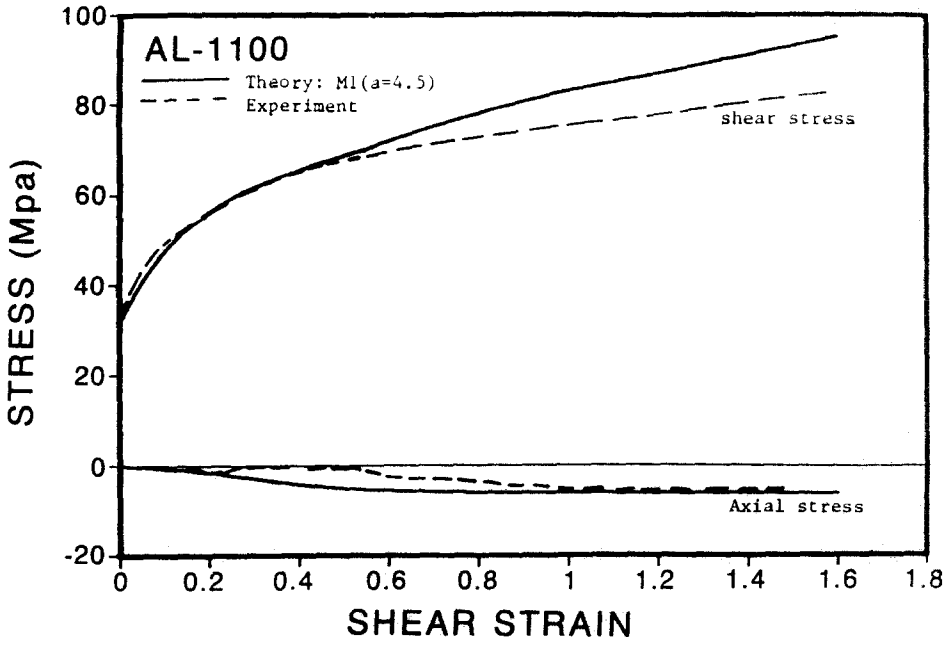

Fig. 3. Axial (and shear) stress development during torsion of Al-1100 cylindrical bars.

$$\sigma = 31 - 12e^{-0.61\epsilon} \quad \text{(Ksi)} ,$$

$$\sigma = 50 + 960\,\epsilon^{0.65} \quad \text{(MPa)} , \tag{72}$$

$$\sigma = 55 + 117\,\epsilon^{0.45} \quad \text{(MPa)} ,$$

respectively. The appropriate values of the dimensionless rotational parameter a for each set of data are listed in the corresponding Figs. 1-3.

V. APPENDIX ON PLASTIC HETEROGENEITY

We conclude the presentation of this new approach to plastic deformation by addressing the fascinating problem of heterogeneity of plastic flow. Three topics of current interest are considered: persistent slip bands, shear bands and Portevin-Le Chatelier bands. The results are briefly presented in a condensed manner and more details will be included in forthcoming papers by WALGRAEF & AIFANTIS [1987b] and ZBIB & AIFANTIS [1987b]. The particular issues we are addressing here are the wavelength of persistent slip bands, the width of shear bands and the velocity of Portevin-Le Chatelier bands. It is noted that each one of the above features cannot be captured by existing theoretical models. In contrast, the present approach provides estimates which compare very well with the experimental data, as it will be seen below.

V.1 *Persistent slip bands*

It is routinely observed during cyclic loading of monocrystals, as well as polycrystalline specimens, that several persistent slip bands (PSBs) are formed which are directly

associated with the occurrence of extrusions/intrusions and nucleation of surface cracks. A PSB consists of a number of slip planes, for example, 5000 in copper, forming a flat lamella which may transverse the whole specimen. The experimental work indicates that only dislocations with the Burgers vector of the primary slip system are required for the formation of a PSB. The dislocations are well ordered. In fact, a periodic arrangement of long dislocation walls subdivides the PSB lamella into channels as shown in Fig. 4a. The walls are oriented perpendicular to the effective Burgers vector and consist of edge dislocation dipoles as shown in Fig. 4b. The dislocation density in the walls is rather high of the order of 10^{15} m^{-2} and details of the arrangement are difficult to analyze. In copper crystals fatigued at room temperature the mutual distance d between the walls and the wall thickness are about 1.3 and 0.15 μm, respectively. A low density of dislocations of the order of 10^{13} m^{-2} having mainly screw character is observed in the channels. The PSBs do not evolve within a uniform region but are embedded within an also patterned structure, commonly known as matrix or vein structure. This structure also consists of dense multipolar bundles separated by dislocation poor regions, also called channels. The width of both the veins and the channels of the matrix is of the order of 1.2 μm and the dislocation density is of the order of 10^{15} m^{-2} in the veins and 10^{11} m^{-2} in the channels.

A preliminary analysis is given next for a system of coupled nonlinear differential equations which we use as a simplified model describing the collective behavior of dislocations during PSB formation. We will show that this model correctly predicts the periodic structure of the ladders and estimates reasonably well the magnitude of its intrinsic wavelength. Moreover, it shows that both a patterning instability associated with the PSB formation, as well as a temporal instability associated with strain bursts, are possible to occur (see also AIFANTIS [1986a]). Additional physical facts for the problems of persistent slip bands and strain bursts can be found respectively in MUGHRABI [1981] and NEUMANN [1968], as well as in related metal physics literature quoted therein.

Motivated by the physical picture discussed earlier, we confine attention to one dimension, say x, associated with the slip direction. We also distinguish between two types of dislocation populations: "trapped" or immobile ones of density ρ_1 making up eventually the wall structure and "free" or mobile ones of density ρ_2 travelling within the channels under the action of a sufficiently high stress intensity. We also assume that the dislocation population is sufficiently high to be represented by continuous concentration fields on a space scale larger than a few lattice spacings. Then, by employing the structure of the dislocation framework outlined in Section II (see also AIFANTIS [1986a]), we can arrive at the following set of coupled differential equations for the trapped or immobile ρ_1 and free or mobile ρ_2 dislocation densities

$$\begin{aligned} \partial_t \rho_1 &= D_1 \nabla_{xx}^2 \rho_1 + g(\rho_1) - h(\rho_1, \rho_2) \ , \\ \partial_t \rho_2 &= D_2 \nabla_{xx}^2 \rho_2 + h(\rho_1, \rho_2) \ , \end{aligned} \tag{73}$$

where ∂_t denotes partial derivative with respect to time and ∇_x means partial derivative with respect to space. The source term $g(\rho_1)$ represents the production/annihilation of the immobile dislocation state ρ_1 before the stress reaches a sufficiently high level to liberate fast moving dislocations comprising the mobile dislocation state ρ_2. The source term $h(\rho_1, \rho_2)$ represents the dislocation reactions occurring after the mobile state comes into play, such as the breaking free of immobile dislocations, as well as the capturing and pinning of mobile dislocations by immobile dipoles and multipoles. It turns

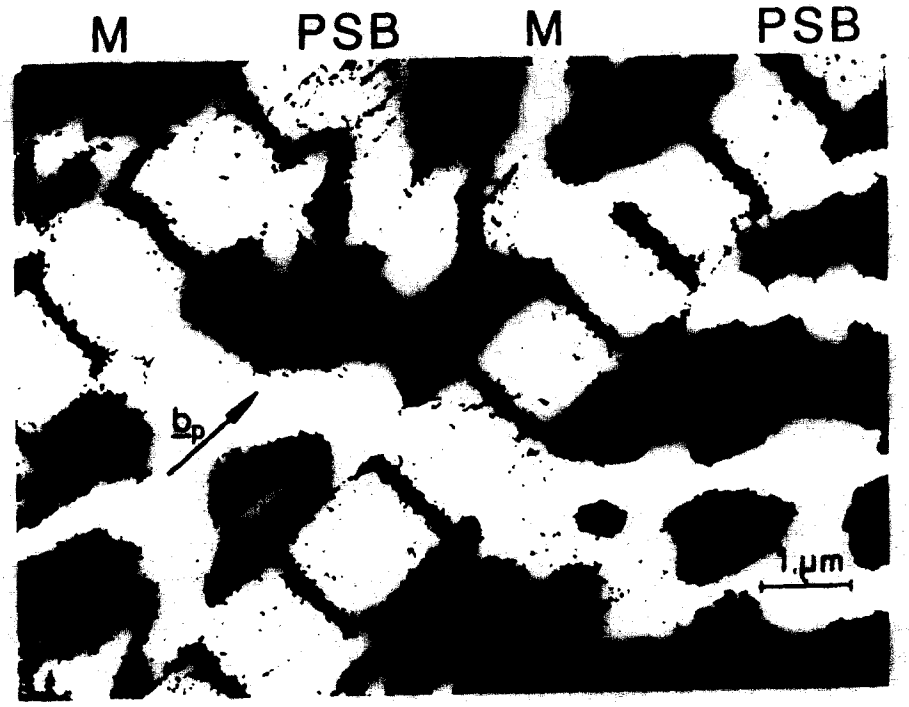

(a)

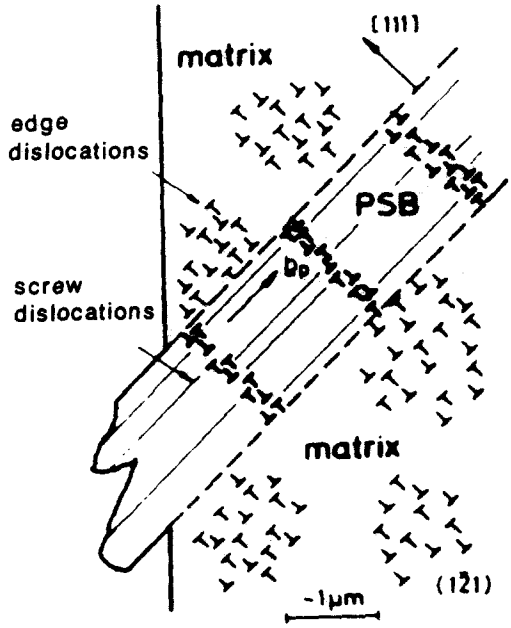

(b)

Fig. 4. (a) Transmission electron microscopy picture showing the periodic structure of the persistent slip bands (PSB) embedded within the matrix (M) region. (b) Schematic picture of PSB and matrix formation illustrating the dislocation substructure and the development of an extrusion. [After Mughrabi and co-workers]

out (AIFANTIS [1986a]) that the motion of dislocations in both the trapped and free states can be modelled by diffusion-like terms $D_1\nabla^2_{xx}\rho_1$ and $D_2\nabla^2_{xx}\rho_2$, where the diffusion-like coefficients D_1 and D_2 are such that $D_1 \ll D_2$. In fact, the diffusivity D_1 measures random-like effects such as interaction with vacancies, thermal events and bowing movements due to local internal stresses. Unlike the Brownian-like nature of D_1, the diffusivity D_2 models the drift-like motion of dislocations liberated by the applied stress (AIFANTIS [1986a]).

The source term $g(\rho_1)$ associated with the immobile state is not necessary to be assigned any specific form. The source term $h(\rho_1,\rho_2)$, however, modelling the interaction between immobile and mobile states, is assumed here to have the form

$$h(\rho_1,\rho_2) = b\rho_1 - c\rho_2\rho_1^2 \ . \tag{74}$$

The coefficient b measures the rate with which immobile dislocations break free when the applied stress exceeds a certain threshold. Finally, the coefficient c measures the pinning rate of freed dislocations by immobile dipoles.

Next, we introduce scaled quantities

$$\rho_1 \to \sqrt{c}\rho_1 \ , \quad \rho_2 \to \sqrt{c}\rho_2 \ , \quad g(\rho_1) \to \sqrt{c}\, g\left(\frac{\rho_1}{\sqrt{c}}\right) \ , \tag{75}$$

so that (73) with the aid of (74) gives the following system of coupled reaction-diffusion equations

$$\begin{aligned} \partial_t\rho_1 &= D_1\nabla^2_{xx}\rho_1 + g(\rho_1) - b\rho_1 + \rho_2\rho_1^2 \ , \\ \partial_t\rho_2 &= D_2\nabla^2_{xx}\rho_2 + b\rho_1 - \rho_2\rho_1^2 \ . \end{aligned} \tag{76}$$

The homogeneous steady-state solution of (76) is given by

$$g(\rho_1^0) = 0 \ , \quad \rho_1^0\rho_2^0 = b \ , \tag{77}$$

and small perturbations from it of the form

$$\tilde{\rho}_1 = \rho_1 - \rho_1^0 \ , \quad \tilde{\rho}_2 = \rho_2 - \rho_2^0 \tag{78}$$

are shown to satisfy the matrix equation

$$\partial_t \begin{bmatrix} \rho_1 \\ \rho_2 \end{bmatrix} = \begin{bmatrix} D_1\nabla^2_{xx} + b + g'(\rho_1^0) & \rho_1^{02} \\ -b & D_1\nabla^2_{xx} - \rho_1^{02} \end{bmatrix} \begin{bmatrix} \rho_1 \\ \rho_2 \end{bmatrix} \ , \tag{79}$$

where the tildes ~ were dropped for convenience. Taking the Fourier transform in (79), defined as usual by

$$\rho_q \sim \int_{-\infty}^{\infty} \rho(x)e^{iqx}dx \ , \tag{80}$$

and setting $g'(\rho_1^0) = -a$ (<0 for the stability of homogeneous states), we can show that, in Fourier space, (79) becomes

$$\partial_t \begin{pmatrix} \rho_{1q} \\ \rho_{2q} \end{pmatrix} = \begin{bmatrix} b - a - q^2 D_1 & \rho_1^{02} \\ -b & -\rho_1^{02} - q^3 D_2 \end{bmatrix} \begin{pmatrix} \rho_{1q} \\ \rho_{2q} \end{pmatrix} \tag{81}$$

The stability of (81) is determined by the characteristic equation

$$\omega^2 + \beta\omega + \gamma = 0 \ , \tag{82}$$

where

$$\begin{aligned} \beta &= -\mathrm{tr}[\quad] = q^2(D_1 + D_2) + (a - b + \rho_1^{02}) \ , \\ \gamma &= \det[\quad] = q^4 D_1 D_2 + q^2[D_2(a - b) + D_1\rho_1^{02}] + a\rho_1^{02} \ . \end{aligned} \tag{83}$$

The homogeneous solution (ρ_1^0, ρ_2^0) becomes unstable when the real part of at least one of the roots of (83) vanishes. Indeed, there are two possible types of instabilities:

(a) A *Hopf bifurcation* leading to homogeneous temporal oscillations occurs for

$$q = 0 \ ; \quad b \geq b_c^0 \equiv a + \rho_1^{02} \ . \tag{84}$$

(b) A *Turning instability* leading to spatially periodic solutions occurs for

$$q = q_c = \left[\frac{a\rho_1^{02}}{D_1 D_2}\right]^{1/4} \ ; \quad b \geq b_c \equiv \left[a^{1/2} + \rho_1^0\left(\frac{D_1}{D_2}\right)^{1/2}\right]^2 \ . \tag{85}$$

As discussed earlier, the first type of instability, which gives oscillations in time, has been experimentally observed in the form of strain bursts for slow increases of stress intensity or low creation rates of dislocations. The second type of instability, which gives spatial patterning, corresponds to the ladder structure of PSBs experimentally observed for sudden increases of stress intensity or high creation rates of dislocations. It generates, in fact, a preferred wavelength λ_c (corresponding to the critical wave number $q_c = 2\pi/\lambda_c$) given by the expression

$$\lambda_c = 2\pi\left[\frac{D_1 D_2}{a\rho_1^{02}}\right]^{1/4} \ . \tag{86}$$

It also turns out by comparing (84) and (85) that the patterning instability is reached before the temporal oscillations when $b_c < b_c^0$, that is when

$$\frac{D_1}{D_2} < \frac{a}{\rho_1^{02}}\left[\left(1 + \frac{\rho_1^{02}}{a}\right)\right]^{1/2} - 1\Bigg]^2 \ . \tag{87}$$

Since it could be argued that in most cases $D_1 \ll D_2$, it may be expected that PSB structures should form before the occurrence of strain bursts.

Before we proceed with the evaluation of (86), it is necessary to recall a microscopic formula for the diffusivity D_2 of the mobile state. This is obtained by further distinguishing between positive and negative dislocations (see, for example, AIFANTIS [1986a]) and reads

$$D_2 = \frac{v^2}{2\rho_1^{02}} \ . \tag{88}$$

Similarly, an estimate for the diffusivity D_1 is needed. This is obtained by recalling the linearized counterpart of $(76)_1$, i.e.

$$\partial_t \rho_1 = D_1 \nabla_{xx}^2 \rho_1 - a\rho_1 \ , \tag{89}$$

whose steady-solution

$$\rho_1 \sim e^{-\sqrt{a/D_1}x} \ , \tag{90}$$

provides an estimate for the ratio (D_1/a) by identifying it with the annihilation length l_1 of dislocation dipoles, i.e.

$$\sqrt{\frac{D_1}{a}} \sim l_1 \simeq 1.6 \times 10^{-9} \text{ m} \quad \text{for Cu} \ . \tag{91}$$

Next we recall Orowan's expression for the plastic strain rate

$$\dot{\epsilon}^p = \tfrac{1}{2}|b|\rho_2^0 v \ , \tag{92}$$

where $|b|$ denotes the magnitude of Burgers vector (in order to distinguish it from the coefficient b), as well as condition $(77)_2$ for the homogeneous distributions.

Upon direct combination of all these formulas we obtain the estimates‡

$$q_c \simeq \left(\frac{|b|}{l_1}\right)^{1/2} \sqrt{\rho_1^0} \to \lambda_c \simeq 2\pi \left(\frac{l_1}{|b|}\right)^{1/2} \frac{1}{\sqrt{\rho_1^0}} \ , \tag{93}$$

which, with l_1 estimated from (91) and a typical value for the Burgers vector magnitude $|b| \simeq 2.55 \times 10^{-10}$ m, gives

$$\lambda_c \simeq d \simeq \frac{16}{\sqrt{\rho_1^0}} \Rightarrow \rho_1^0 \simeq \frac{256}{d^2} \ . \tag{94}$$

Relation $(94)_2$ is consistent with many experimental observations suggesting that the wavelength of periodic dislocation structures (including cell walls) is inversely proportional to the square root of the dislocation density. For the case of the ladder structure of PSBs, in particular, it is worth noting that empirical modelling and observations have resulted in a formula identical to $(94)_2$ with 256 replaced by 280.

The previous discussion was based on the assumption that the nonlinear interaction between mobile and immobile dislocations is of the form given by (74). This means that

‡The symbol $\simeq$ in eqns (93) and (94) denotes equality within a scalar multiple, which in the case of $(93)_2$ turns out to be $(\sqrt{2}\dot{\epsilon}^p/b)^{1/2}$, provided that the coefficient b is taken proportional to the plastic strain rate $\dot{\epsilon}^p$.

immobile dislocations are freeing at the rate $b\rho_1$ to be subsequently trapped at a pinning rate $c\rho_2\rho_1^2$ by immobile dipoles. Of course this is only a working hypothesis and, in general, it is expected that tripoles, quadropoles and dislocation multipoles will participate in the process. In a preliminary effort we examined (WALGRAEF & AIFANTIS [1987]), the case where $h(\rho_1,\rho_2)$ is thus given, instead of (74), by the generalized form

$$h(\rho_1,\rho_2) = b\rho_1 - \sum_n c_n\rho_1^n\rho_2 \ , \tag{95}$$

where the index n models the order of reaction. It was found that the effective diffusivity D_2 in (88) is now given by

$$D_2 = \frac{v^2}{2(\Sigma c_n \rho_1^{0n})} \ , \tag{96}$$

where the sum Σ extends over n. It turns out that for $n = 1$ there is no instability but damped propagation of inhomogeneities. The case $n = 2$ was discussed above. For the case where $n > 2$, it turns out that there is no qualitative change of the behavior of the model equations. In fact, an initial analysis shows that all previous results pertaining, for example, to the characterization of the instability and the wavelength are identically valid provided that we formally set

$$b \to \bar{b} = b\left(\rho_1^0 \frac{\partial ln\bar{c}}{\partial \rho_1^0} - 1\right) \ , \quad c \to \bar{c} = \frac{1}{\rho_1^{02}} \Sigma c_n \rho_1^{0n} \ . \tag{97}$$

V.2 *Shear bands*

Although the problem of localization of plastic flow in small but finite size deformation zones, commonly known as shear bands (SBs), has been extensively discussed in the last ten years or so, most of the theoretical results were concerned with the onset of instability and the determination of the angle and critical loads at which a shear band occurs. No theory has been proposed which can successfully account for the structure and evolution of the band in the postlocalization regime. For a brief review of the subject from the viewpoint of the inability of existing theories to capture postlocalization features such as band width, the reader can consult the recent paper by TRIANTAFYLLIDIS & AIFANTIS [1986]. It was, in fact, in that paper where the problem of shear band width for hyperelastic materials was addressed by including higher-order deformation gradients into the strain energy function. This gradient approach to the problem of localization of deformation was directly motivated by earlier work on fluid microstructures and phase transition theory as discussed by AIFANTIS [1984, 1985].

The problem of shear band width in plastic materials will be addressed in detail in a forthcoming publication by ZBIB & AIFANTIS [1987b]. However, we outline below a summary of the analysis as it applies to incompressible rigidly plastic materials satisfying the equations

$$\text{div}\,\mathbf{S} = 0 \ ; \quad \mathbf{S} = -p\mathbf{1} + 2\mu\mathbf{D} \ , \quad \mu = \tau/\dot{\gamma} \ , \tag{98}$$

with $\tau = (\frac{1}{2}\mathbf{S}'\cdot\mathbf{S}')^{1/2}$, $\dot{\gamma} = (2\mathbf{D}\cdot\mathbf{D})^{1/2}$, and $\text{tr}\,\mathbf{D} = 0$.

The point of departure of the present proposal from previous ones is the assumption

that the flow stress τ is not a function of the plastic strain $\gamma = \int_0^t \dot{\gamma} \mathrm{d}t$ only, but also of its gradients. A partial motivation for such an assumption (see also COLEMAN & HODGDON [1985]), which here is taken to be of the form (with c a positive constant)

$$\tau = \tau(\gamma) - c\nabla^2\gamma \ , \tag{99}$$

can be found in AIFANTIS [1985].

The onset of instability can be determined by employing a standard perturbation analysis similar to that used in the previous section. We thus assume that the velocity field admits the representation

$$\mathbf{v} = \mathring{L}\mathbf{x} + \epsilon[\hat{v}\exp(iqz + \omega t)]\boldsymbol{\nu} \ , \tag{100}$$

with $z = \mathbf{n}\cdot\mathbf{x}$, $(\mathring{\mathbf{L}}, \hat{v})$ being constants, $(\mathbf{n}, \boldsymbol{\nu})$ denoting, respectively, unit vectors perpendicular and parallel to the band, (q, ω) signifying respectively wave number and speed of growth and ϵ being a small positive number ($\epsilon \ll 1$). In writing (100) we have also tacitly assumed plane strain conditions ($D_{11} = -D_{22}$, $D_{33} = 0$) with the direction of plastic flow being parallel to the shear band direction $\boldsymbol{\nu}$. Then we have $(\nu_1, \nu_2) = (n_2, -n_1) = (\cos\theta, \sin\theta)$, where θ is the angle between the band direction and the x_1-axis [$\mathbf{x} = (x_1, x_2, x_3)$] also assumed here to coincide with the appropriate principal direction of $\mathring{\mathbf{D}}$. On assuming an expansion for the pressure field p similar to that of eqn (100) and then substituting the results in (98), we obtain the onset of localization condition

$$\mathrm{tr}\{[\mu\mathbf{1} + m(\mathbf{Dn} \otimes \mathbf{Dn})](\boldsymbol{\nu} \otimes \boldsymbol{\nu})\} = 0 \ , \tag{101}$$

where[§] $m \equiv 4(h - cq^2 - \mu\omega)/\omega\dot{\gamma}^2$ and the superscript ^{0} has been dropped for convenience. Under the plane strain conditions discussed earlier, eqn (101) yields

$$\omega = -(h + cq^2)/\mu\cot^2 2\theta \ , \tag{102}$$

suggesting that the preferred or critical conditions for the instability to occur are*

$$\theta = \pi/4 \ , \quad h \leq 0 \ , \tag{103}$$

both of which are familiar from classical considerations, even though derived here with a different method most suited for the subsequent postlocalization analysis.

Having the direction of the band thus obtained from linear stability analysis, the band width can now be determined from a nonlinear analysis of an essentially one-dimensional problem for the plastic strain distribution in the direction perpendicular to the band. In fact, by assuming now for the velocity field, instead of the linear perturbation expansion (100), the nonlinear steady-state representation

$$\mathbf{v} = \mathring{L}\mathbf{x} + f(z)\boldsymbol{\nu} \ , \tag{104}$$

[§]It is noted that in this particular subsection $h = \mathrm{d}\tau/\mathrm{d}\gamma$ denotes the hardening modulus in shear while in other parts of the paper $h = \mathrm{d}\bar{\sigma}/\mathrm{d}\bar{\epsilon}$ measures the hardening in tension.

*It is shown elsewhere that these conditions suggest the introduction of higher-order gradients in eqn (99) in order for the linearized theory to provide a definite wavelength.

where $f(z)$ is a shape factor representing the intensity of deformation and structure of the localized zone in the direction $z = \mathbf{n}.\mathbf{x}$ perpendicular to the band, it follows from (104) that

$$\mathbf{D} = \mathring{\mathbf{D}} + g(z)\mathbf{M} \; ; \quad g(z) = f'(z) \; , \tag{105}$$

suggesting that in the $(\boldsymbol{\nu}, \mathbf{n})$ coordinate system, the mode of deformation is simple shearing in the x-z plane. Thus, all components of the strain rate $\mathbf{D}$ but $D_{zx} = D_{xz} = \mathring{D}_{xz} + 1/2\, g(z)$ are uniform (equal to $\mathring{D}_{ij}$). It follows that all components of the stress $\mathbf{S}$ but $S_{zx} = S_{xz} = \mathring{S}_{xz} + \mu g(z)$ are also uniform (equal to $\mathring{S}_{ij}$). Then the only component of the equilibrium equations $(98)_1$ nontrivially satisfied implies

$$\frac{\partial \tau}{\partial z} = 0 \; , \tag{106}$$

which in conjunction with (99) gives by integration

$$c\gamma_{zz} = \tau(\gamma) - \tau_0 \; , \tag{107}$$

where $\tau_0 = \tau(t)$ denotes a constant of integration [equal to the stress applied at the boundary] and $\tau(\gamma)$ is a softening type graph [admitting condition $(103)_2$] as shown in Fig. 5a.

The solution of (107) for $-\infty < z < \infty$ can readily be obtained by using the methods advanced by Aifantis and Serrin as quoted in AIFANTIS [1984] (see also TRIANTAFYLLIDIS & AIFANTIS [1986]). It reads

$$z = \bar{z} + \int_{\gamma(\bar{z})}^{\gamma(z)} \left\{ \frac{2}{c} \int_{\gamma_1}^{\gamma} [\tau(\gamma) - \tau_0] \mathrm{d}\gamma \right\}^{-1/2} \mathrm{d}\gamma \; , \tag{108}$$

where $\bar{z}$ is an arbitrary point and $\gamma_1[\tau_0 = \tau(\gamma_1)]$ is the shear strain at $z = \pm\infty$. The representation (108) is valid for $-\infty \leq z \leq z^*$ and is symmetric about z^*, with z^* denoting the point where the graph $\gamma = \gamma(z)$ has a maximum $\gamma_2 = \gamma(z^*)\,[\gamma_z(z^*) = 0]$. Moreover, it turns out that the triplet $(\tau_0, \gamma_1, \gamma_2)$ must satisfy the following area condition (also shown in Fig. 5a)

$$\int_{\gamma_1}^{\gamma_2} [\tau(\gamma) - \tau_0] \mathrm{d}\gamma = 0 \; , \tag{109}$$

in order for the solution (108) of eqn (107) to exist. Pictorially, the representation (108) is shown in Fig. 5b.

The physical meaning of the solution (108) in connection with the growth of shear bands in rigidly plastic materials is discussed by ZBIB & AIFANTIS [1987b]. Roughly speaking, as soon as the applied shear $\gamma_1 = \gamma_1(t)$ falls within the unstable region of negative slope, $\gamma > \gamma_m$, in Fig. 5b, homogeneous deformations cease to exist and a nonuniform solution of the form (108), with $\gamma_1 < \gamma_m$ and $\gamma_2 > \gamma_m$, sets in. As condition (109) has to be satisfied, increase of the shear intensity γ_2 within the band implies a decrease of the applied strain γ_1 ($\dot{\gamma}_1 < 0$, unloading). Such unloading is not permitted, however, by the present rigid plastic model and thus γ remains constant in the respective regions. Since $\gamma_1 = \gamma_1(t)$ enters as a parameter in (108), we may view it as

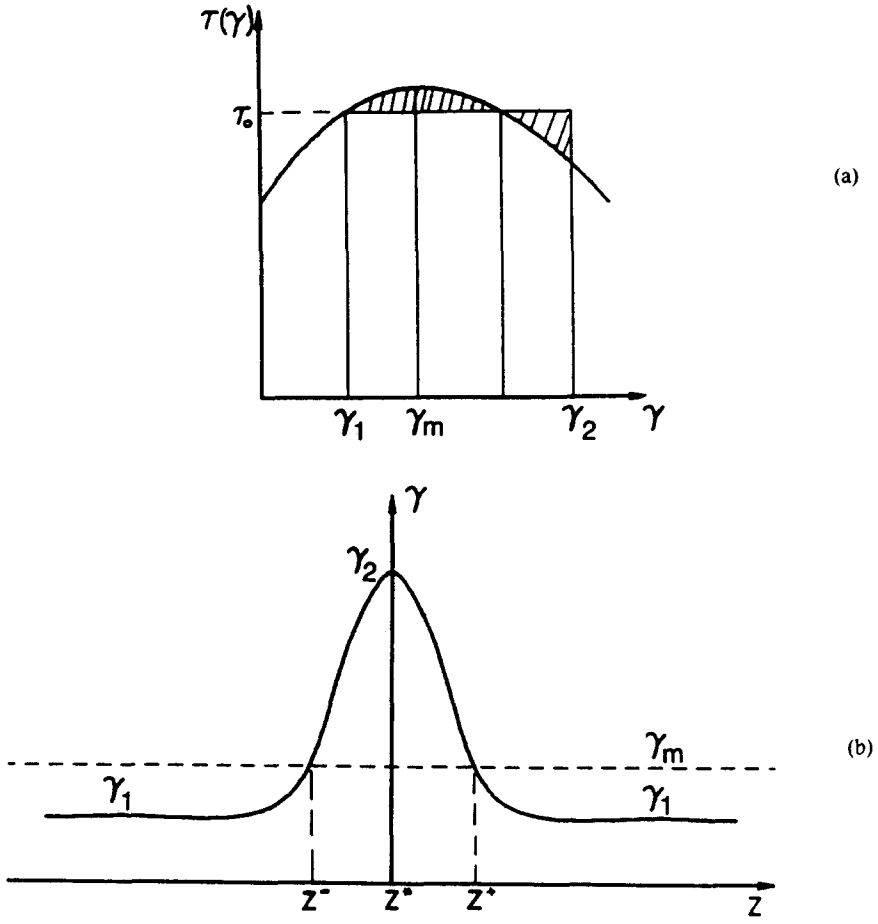

Fig. 5. (a) Schematic softening type stress-strain relation and the equal area rule. (b) Schematic distribution of shear strain in the direction perpendicular to the band.

a time-like variable to be used in order to describe the growth of plastic strain within the band. In fact, the condition $\partial\gamma/\partial\gamma_1 = 0$ determines two points $z^{\pm}$ symmetric with respect to z^*. In the interval $z^- \leq z \leq z^+$ where $\partial\gamma/\partial\gamma_1 \leq 0$ the strain profile is continuously determined by an iterative procedure through (108) while in the region outside the interval (z^-, z^+) where $\partial\gamma/\partial\gamma_1 \geq 0$ the strain profile is fixed again through (108) once such a profile sets in. The details of such a construction, which is different than the one outlined by COLEMAN & HODGDON [1985], can be found in a forthcoming article by ZBIB & AIFANTIS [1987b].

In the same article a comparison is made between the presently outlined procedure and that proposed by COLEMAN & HODGDON [1985] for a very special class of materials for which

$$\tau(\gamma) = \tau_m - \alpha(\gamma - \gamma_m)^2 \,, \tag{110}$$

where α, γ_m and τ_m are constants. It then turns out (ZBIB & AIFANTIS [1987b]) that the distribution of shear strain γ is given by

$$\gamma = \begin{cases} \gamma_m + \delta\left[3\operatorname{sech}^2\left(\sqrt{\frac{2\alpha\delta}{c}}\,\frac{z-\bar{z}}{2}\right) - 1\right] \; ; \quad z^- \le z \le z^+ \, , \\ \gamma_m + \dfrac{0.89c}{\alpha(z-\bar{z})^2} \; ; \quad z < z^- \, , \quad z > z^+ \, , \end{cases} \tag{111}$$

while the shear band width $w = z^+ - z^-$ is given by

$$w = 1.46\sqrt{\frac{c}{\alpha\delta}} \, , \tag{112}$$

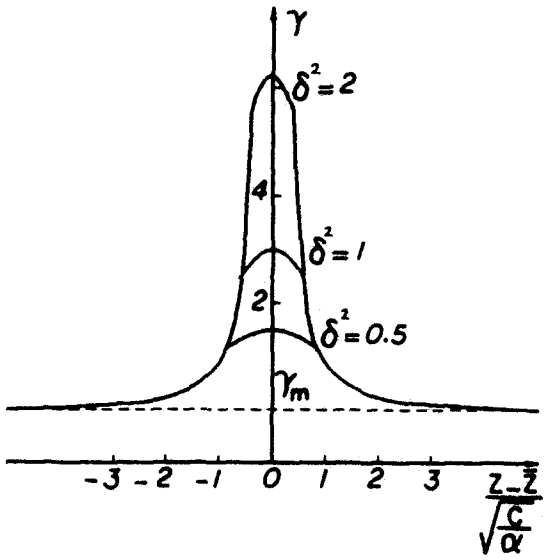

(a)

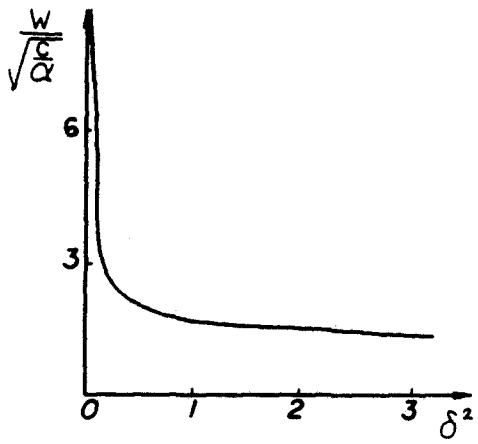

(b)

Fig. 6. (a) Numerical results illustrating the shear distribution and the structure of the band. (b) The variation of the shear band width with the strain parameter δ.

where the parameter δ was defined for convenience as $\delta = \gamma_m - \gamma_1$. Figures 6a and 6b, which are discussed in detail by ZBIB & AIFANTIS [1987b], give respectively the distribution of the shear strain as determined by (111) and the width of the shear band as determined by (112).

V.3 *Portevin-Le Chatelier bands*

In this concluding section we report some rather impressive preliminary results pertaining to the structure and propagation of the Portevin-Le Chatelier (PLC) bands. Roughly speaking, the PLC effect consists of a repeated propagation of deformation bands along a tensile specimen subjected to a constant strain or stress rate. This is accomplished by the appearance of abrupt stress drops or steps on the deformation curves, as is pictorially shown in Fig. 7a. The effect is found at slightly elevated temperatures in mild steel and at room temperature in several dilute alloys including Al, Cu, Ni and Fe alloys. More details on the physics of PLC effect can be found in recent

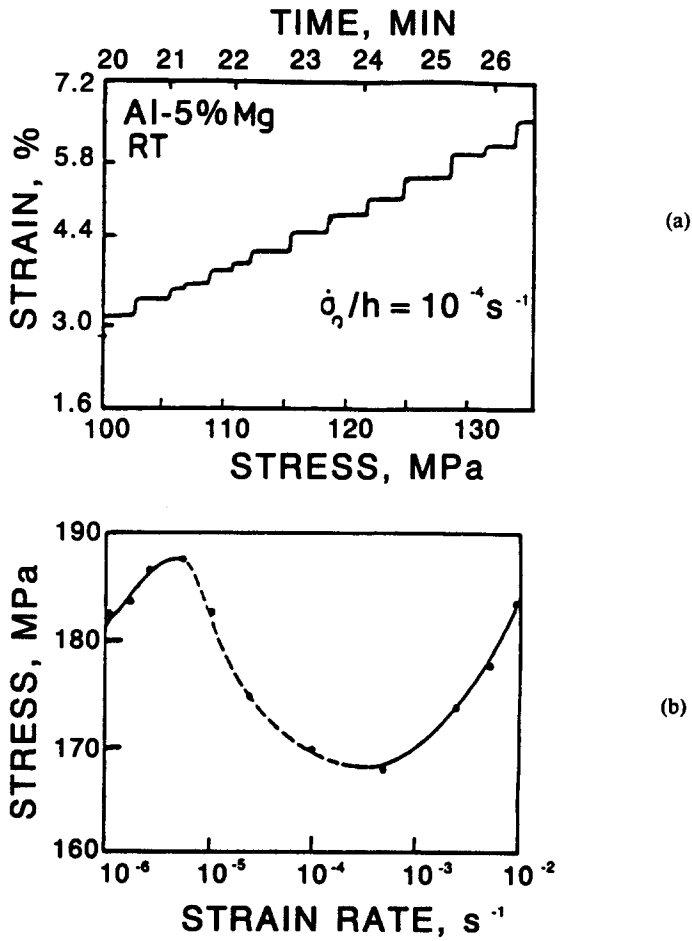

Fig. 7. (a) Experimental staircase stress-strain curve for Al-5% Mg. (b) Experimental loop-type stress-strain rate curve for Al-5% Mg. [After Kubin and co-workers]

papers by ESTRIN & KUBIN [1986], KUBIN *et al.* [1986] as well as references quoted therein.

The PLC effect is associated with the nonlinear dependence of the flow stress on the strain rate; in fact, the nonconvexity due to the concurrence of a negative strain rate sensitivity, as shown pictorially in Fig. 7b. In a series of papers by Estrin and Kubin an attempt was made to discuss the PLC effect on the basis of a constitutive equation of the form

$$\sigma = h\epsilon + f(\dot{\epsilon}) \ , \tag{113}$$

where, σ, ϵ and $\dot{\epsilon}$ denote as usual one-dimensional stress, strain and strain rate, respectively; the hardening rate h is assumed constant and the function f, being essentially of the loop-type depicted in Fig. 7b, takes into account the strain rate dependent interaction between mobile dislocation and localized obstacles. On the basis of (113) and qualitative stability arguments Estrin and Kubin were able to speculate the profile of the PLC bands as they propagate in the form of travelling waves along the specimen. Figure 8 is indeed extracted from their paper and shows schematically the situation as they expect it. Their preliminary analysis, of course, predicted neither the speed of the bands nor their width.

A simple quantitative explanation of the situation can be given if the problem is reformulated within the present dislocation framework. Roughly speaking, this amounts to replacing eqn (113) by

$$\sigma = h\epsilon + f(\dot{\epsilon}) + c\epsilon_{xx} \ , \tag{114}$$

where the last term models the strongly inhomogeneous character of dislocation distribution as it manifests itself in the form of strain gradients. The coefficient c is taken as constant for simplicity. For constant stress rate tests ($\sigma = \dot{\sigma}_0 t$) and by denoting the homogeneous steady-state solution of (114) by $\dot{\epsilon}_s$, we have

$$\dot{\sigma}_0 = h\dot{\epsilon}_s \tag{115}$$

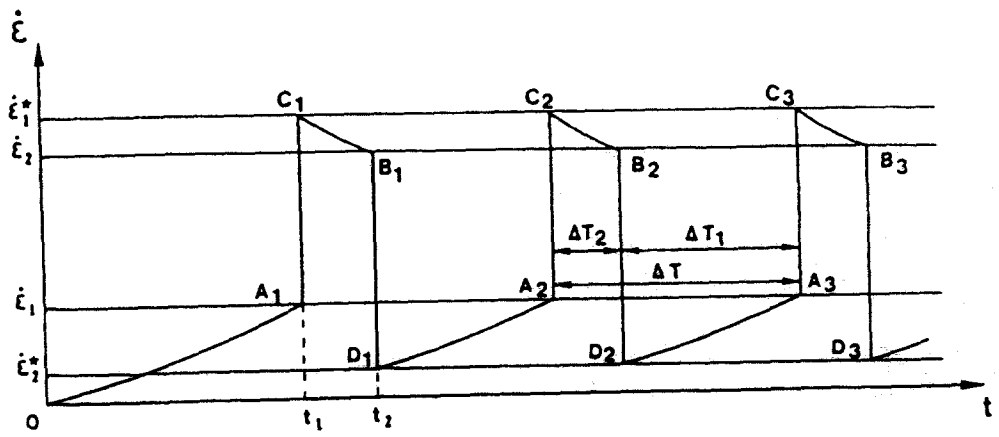

Fig. 8. Schematic representation of PLC bands as proposed by Estrin and Kubin on the basis of qualitative arguments.

Next, we search for travelling wave solutions of the form

$$\dot{\epsilon} = z(Vt - x) \ , \tag{116}$$

and also make use of the normalized variable

$$\eta = \sqrt{\frac{h}{c}}\,(Vt - x) \ . \tag{117}$$

Then, by also defining $\mu = V/\sqrt{ch}$, (114) implies

$$z_{\eta\eta} + \mu f'(z) z_\eta + (z - z_s) = 0 \ , \tag{118}$$

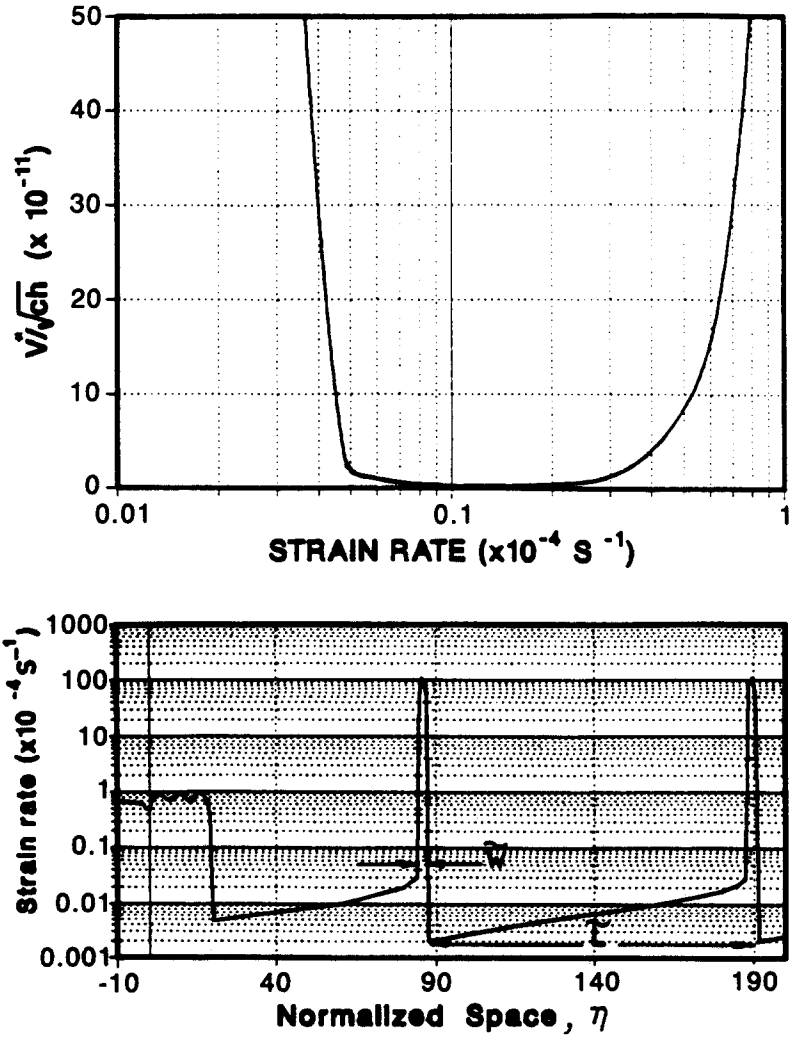

Fig. 9. (a) Predicted variation of the band velocity with the applied strain rate. (b) Predicted periodic structure of the Portevin-Le Chatelier bands.

which is a nonlinear differential equation of Lienard's type. It can be shown that a unique stable periodic solution exists and that the natural speed of the travelling wave is given by the expression

$$V^* = \frac{2\sqrt{ch}}{f'(z_s)} \,. \tag{119}$$

Moreover, the width of the band can be explicitly calculated.

More details on this problem can be found in a forthcoming article by ZBIB & AIFANTIS [1987b]. In fact, Figs. 9a and 9b are extracted from their numerical analysis. They show the dependence of the velocity of the band V^* on the applied strain rate and the profile of the strain rate as a function of the wave variable η ($\tilde{w}$ denotes a properly normalized band width and $\tilde{L}$ the period). Similarly, Figs. 10a and 10b respectively show

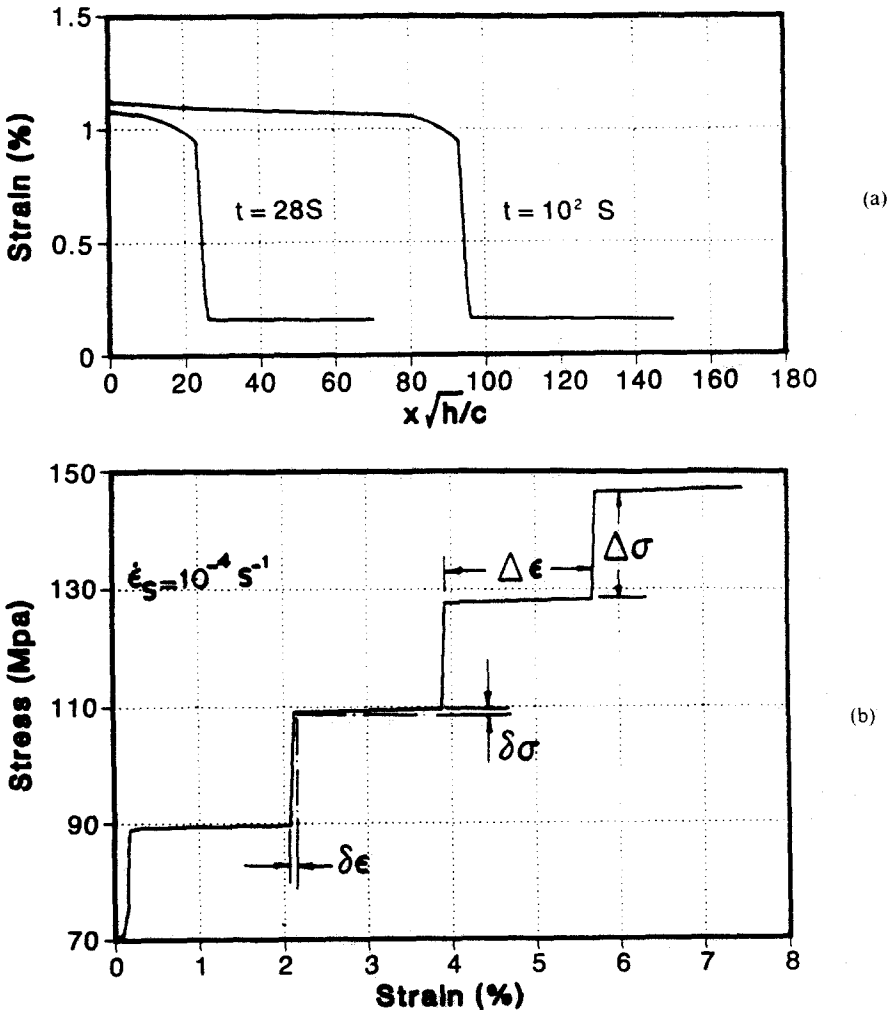

Fig. 10. (a) Predicted strain profile in the PLC regime. (b) Predicted staircase stress-strain curve in the PLC regime.

the strain distribution with respect to a normalized space variable in two different instances and the predicted staircase stress–strain profile.

Acknowledgement—The support of the National Science Foundation and the hospitality of the Naval Research Laboratory in Washington, D.C., is appreciated. Discussions with my student, H. Zbib, and my colleagues, D. Walgraef and Y. Dafalias, are also acknowledged.

NOTE ADDED IN PROOF

This article was invited and originally scheduled for the "Phillips Memorial Issue," earlier published in this journal; but, unfortunately, it was not completed in time. It does not attempt to review ongoing progress in plasticity and localization of deformation theories. It presents, instead, results either recently obtained or currently being completed by the author and his co-workers.

Naturally, only the basic elements of this rather new approach to plastic flow were outlined and more details can be found in either recently published or forthcoming articles as listed in the references. In this connection, many current and excellent papers on different "micromechanics" approaches to large plastic deformation theories (e.g. Asaro, Havner, and their co-workers) are not quoted here. Similarly, numerous outstanding advances are nonlocal and softening behavior (e.g. the earlier work of Eringen and co-workers on nonlocal plasticity and the more recent work of Bazant, Schreyer, Coleman and their co-workers, on localization) are also missing from the list of references. Such a detailed review and comparison of the present method to previous approaches to the heterogeneity of plastic flow will be discussed elsewhere. Nevertheless, it is pointed out here that whereas Eringen's and Bazant's theories are strictly nonlocal (spatial integrals), Schreyer's and Coleman's approaches are pseudo-nonlocal or of a gradient type, similar to the present approach.

However, Schreyer's approach [H.L. SCHREYER and Z. CHEN, J. Appl. Mech., **53**, 791 (1986)] assumes a dependence of the yield condition on the first gradient only, in contrast to the present approach which is heavily based on the second gradient. Coleman's approach [B.D. COLEMAN and M.L. HODGDON, Arch. Rat. Mech. Anal. **90**, 219 (1985)], on the other hand, utilizes the second gradient of strain but not directly in the yield condition or the flow stress, as is the case in the present approach. In this connection, we also point out that the shear bandwidth in the present case of rigid plastic materials was defined by the region where continuous loading occurs. Although this is similar to Coleman et al.'s assumption, our construction does not require their "end" conditions on the second spatial derivative of strain. In any case, such a definition of shear bandwidth may be somewhat ambiguous, especially when comparisons with observations are sought. This problem does not arise, of course, in the definition used by Triantafyllidis and Aifantis (19896) in their treatment of hyperelastic materials.

In conclusion, we also point out that the comparisons between theory and experiment contained in Figs. 1–3 should be viewed only in relation to recent concerns about the appropriateness of existing tension–torsion tests in calibrating "simple shear" large deformation models (due to specimen configuration, precision of available axial-torsional extensiometers, and assurance of specimen homogeneity).

REFERENCES

1952 DRUCKER, D.C. and PRAGER, W., "Soil Mechanics and Plastic Analysis or Limit Design," Quart. Appl. Math., **10**, 157.

1968 NEUMANN, P., "Strain Bursts and Coarse Slip During Cyclic Deformation," Z. Metallkd., **59**, 927.

1969 GILMAN, J.J., Micromechanics of Flow in Solids, McGraw-Hill, New York.
1972 BAILEY, J.A., HAAS, S.L., and NAWAB, K.C., "Anisotropy in Plastic Torsion," J. Basic Engng., **94**, 231.
1975 STOREN, S.S. and RICE, J.R., "Localized Necking in Thin Sheets," J. Mech. Phys. Solids, **23**, 421.
1979 KOSEVICH, A.M., "Crystal Dislocations and the Theory of Elasticity," in NABARRO, F.R.N. (ed.), Dislocations in Solids, Vol. 1, North-Holland, Amsterdam, p. 33.
1981 AIFANTIS, E.C., "Elementary Physicochemical Degradation Processes," in SELVADURAI, A.P.S. (ed.), Mechanics of Structured Media, Elsevier, Amsterdam, p. 301.
1981 BAMMANN, D.J. and AIFANTIS, E.C., "On the Perfect Lattice-Dislocated State Interaction," in SELVADURAI, A.P.S. (ed.), Mechanics of Structured Media, Elsevier, Amsterdam, p. 79.
1981 MUGHRABI, H., "Cyclic Plasticity of Matrix and Persistent Slip Bands in Fatigued Metals," in BRULIN, O. and HSIEH, R.K.T. (eds.), Continuum Models for Discrete Systems 4, North-Holland, Amsterdam, p. 241.
1982 BAMMANN, D.J. and AIFANTIS, E.C., "On a Proposal for a Continuum with Microstructure," Acta Mechanica, **45**, 91.
1982 HART, E.W. and CHANG, Y.W., "Material Rotation Effects in Tension-Torsion Testing,," in WAGONER, R.H. (eds.), Novel Techniques in Metal Deformation Testing, AIME, p. 253.
1982 HIRTH, J.P. and LOTHE, J., Theory of Dislocations, John Wiley, New York.
1982 MURA, T., Micromechanics of Defects in Solids, Martinus-Nijhoff, The Hague.
1982 NAGTEGAAL, J.C. and DE JONG, J.E., "Some Aspects of Non-Isotropic Workhardening in Finite Strain Plasticity," in LEE, E.H. and MALLET, R.L. (eds.), Plasticity of Metals at Finite Strain: Theory, Experiment, and Computation, Stanford University, p. 65.
1983 DAFALIAS, Y.F., "Corotational Rates for Kinematic Hardening at Large Plastic Deformations," J. Appl. Mech., **50**, 561.
1983 LORET, B., "On the Effects of Plastic Rotation in the Finite Deformation of Anisotropic Elastoplastic Materials,," Mech. Mater., **2**, 287.
1984 AIFANTIS, E.C., "On the Microstructural Origin of Certain Inelastic Models," Trans. ASME, J. Eng. Mat. Tech., **106**, 326.
1984 BAMMANN, D.J., "An Internal Variable Model of Viscoplasticity,," in AIFANTIS, E.C. and DAVISON, L. (eds.), Media with Microstructures and Wave Propagation, Int. J. Engng. Sci., Vol. 8-10, Pergamon Press, p. 1041.
1984 DAFALIAS, Y.F., "The Plastic Spin Concept and a Simple Illustration of Its Role in Finite Plastic Transformations," Mech. Mater., **3**, 223.
1984 DRUCKER, D.C., "Material Response and Continuum Relations; or From Microscales to Macroscales," Trans. ASME, J. Engng. Mat. Tech., **106**, 286.
1984 ONAT, E.T., "Flow of Kinematically Hardening Rigid-Plastic Materials," in DVORAK, G.J. and SHIELD, R.T. (eds.), Mechanics of Materials Behavior – Daniel C. Drucker Anniversary Volume, Elsevier Sci. Publ., Amsterdam, p. 311.
1985 AIFANTIS, E.C. and HIRTH, J.P. (eds.), The Mechanics of Dislocations, ASM, Metals Park.
1985 AIFANTIS, E.C., "Continuum Models for Dislocated States and Media with Microstructures," in AIFANTIS, E.C. and HIRTH, J.P. (eds.), The Mechanics of Dislocations, ASM, Metals Park, p. 127.
1985 COLEMAN, B.D. and HODGDON, M.L., "On Shear Bands in Ductile Materials," Arch. Rat. Mech. Anal., **90**, 219.
1985 WALGRAEF, D. and AIFANTIS, E.C., "On the Formation and Stability of Dislocation Structures I, II, III," Int. J. Engng. Sci., **23**, 1351, 1359, 1365.
1986a AIFANTIS, E.C., "On the Dynamical Origin of Dislocation Patterns," Mater. Sci. Eng., **81**, 563.
1986b AIFANTIS, E.C., "Mechanics of Microstructures I, II, III," in BALKRISHNAN, V. and BOTTANI, C. (eds.), Mechanical Properties and Behaviour of Solids-Plastic Instabilities, [ICTP Enrico Fermi School of Theoretical Physics, 12-30 August 1985, Trieste, Italy], World Scientific, Singapore, pp. 314, 332, 347.
1986c AIFANTIS, E.C., "On the Structure of Single Slip and Its Implications to Inelasticity," in GITTUS, J., NEMAT-NASSER, S., and ZARKA, J. (eds.), Physical Basis and Modelling of Finite Deformations of Aggregates, [Proc. International Symposium – JEAN MANDEL in Memoriam, Sept. 30-Oct. 2, 1985, Paris, France], Elsevier Appl. Sci. Publ., Amsterdam, p. 283.
1986 ESTRIN, Y. and KUBIN, L.P., "Micro and Macro Aspects of Unstable Plastic Flow," in AIFANTIS, E.C. and GITTUS, J. (eds.), Phase Transformations, Elsevier Appl. Sci. Publ., Amsterdam, p. 185.
1986 TRIANTAFYLLIDIS, N. and AIFANTIS, E.C., "A Gradient Approach to Localization of Deformation. I. Hyperelastic Materials," J. Elasticity, **16**, 225.
1986 WHITE, C. and ANAND, L., private communication.
1987 DAFALIAS, Y.F. and AIFANTIS, E.C., forthcoming. See also "On the Origin of Plastic Rotations and Spin," Appendix to the article 1986c above. [Also MM Report No. 8, "On the Microscopic Origin of Plastic Spin," Michigan Technological University, Houghton, Michigan.]
1987 KUBIN, L.P., CHIHAB, K., and ESTRIN, Y., "Nonuniform Plastic Deformation and the Portevin-Le Chatelier Effect," in WALGRAEF, D. (ed.), Patterns Defects and Microstructures in Nonequilibrium

Systems (NATO Advanced Workshop held in Austin, TX, March 1986), Martinus-Nijhoff, The Hague.

1987–1988 WALGRAEF, D. and AIFANTIS, E.C., "Plastic Instabilities, Dislocation Patterns, and Nonequilibrium Phenomena," Res. Mechanica, forthcoming.

1987a ZBIB, H.M. and AIFANTIS, E.C., "The Concept of Relative Spin and Its Implications to Large Deformation Theories," Mechanics of Microstructures, MM Report No. 13, Michigan Technological University, Houghton, Michigan. [See also: "Constitutive Equations for Large Material Rotations" in DESAI, C.S. et al. (eds.), Constitutive Laws for Engineering Materials: Theory and Applications, Elsevier Science Publishing, New York.]

1987b ZBIB, H.M. and AIFANTIS, E.C., "On the Postlocalization Behavior of Plastic Deformation," Mechanics of Microstructures, MM Report No. 1, Michigan Technological University, Houghton, Michigan.

Department of Mechanical Engineering and Engineering Mechanics
Michigan Technological University
Houghton, MI 49931

(*Received* 5 *August* 1986; *In revised form* 28 *February* 1987)